Title

Calibration of the carbon isotope composition (δ13C) of benthic foraminifera

Journal

Paleoceanography and Paleoclimatology, 32(6)

ISSN

2572-4517

Authors

Schmittner, Andreas
Bostock, Helen C
Cartapanis, Olivier
et al.

Publication Date

2017-06-01

DOI

10.1002/2016pa003072

Peer reviewed

AGU PUBLICATIONS

Paleoceanography

RESEARCH ARTICLE
10.1002/2016PA003072

Key Points:
- Global comparison of bottom-water and benthic foraminifera (*Cibicides*) carbon isotope ($\delta^{13}C$) data
- *Cibicides* $\delta^{13}C_{Cib}$ reflect sea water dissolved inorganic carbon $\delta^{13}C_{DIC}$
- Carbonate ion and pressure effects impact $\delta^{13}C_{Cib}$

Supporting Information:
- Supporting Information S1
- Figure S1
- Figure S2

Correspondence to:
A. Schmittner,
aschmitt@coas.oregonstate.edu

Citation:
Schmittner, A., et al. (2017), Calibration of the carbon isotope composition ($\delta^{13}C$) of benthic foraminifera, *Paleoceanography*, *32*, 512–530, doi:10.1002/2016PA003072.

Received 9 DEC 2016
Accepted 4 MAY 2017
Accepted article online 12 MAY 2017
Published online 3 JUN 2017
Corrected 12 JUN 2017

This article was corrected on 12 JUN 2017. See the end of the full text for details.

Calibration of the carbon isotope composition ($\delta^{13}C$) of benthic foraminifera

Andreas Schmittner[1], Helen C. Bostock[2], Olivier Cartapanis[3,4], William B. Curry[5,6], Helena L. Filipsson[7], Eric D. Galbraith[4,8,9], Julia Gottschalk[3], Juan Carlos Herguera[10], Babette Hoogakker[11], Samuel L. Jaccard[3], Lorraine E. Lisiecki[12], David C. Lund[13], Gema Martínez-Méndez[14], Jean Lynch-Stieglitz[15], Andreas Mackensen[16], Elisabeth Michel[17], Alan C. Mix[1], Delia W. Oppo[6], Carlye D. Peterson[18], Janne Repschläger[19], Elisabeth L. Sikes[20], Howard J. Spero[18], and Claire Waelbroeck[17]

[1]College of Earth, Ocean, and Atmospheric Sciences, Oregon State University, Corvallis, Oregon, USA, [2]National Institute of Water and Atmospheric Research, Wellington, New Zealand, [3]Institute of Geological Sciences and Oeschger Center for Climate Change Research, University of Bern, Bern, Switzerland, [4]Department of Earth and Planetary Sciences, McGill University, Montreal, Québec, Canada, [5]Bermuda Institute of Ocean Sciences, Bermuda, [6]Department of Geology and Geophysics, Woods Hole Oceanographic Institution, Woods Hole, Massachusetts, USA, [7]Department of Geology, Lund University, Lund, Sweden, [8]Institut de Ciència i Tecnologia Ambientals, Universitat Autònoma de Barcelona, Barcelona, Spain, [9]ICREA, Barcelona, Spain, [10]Oceanología, Centro de Investigación Científica y de Educación Superior de Ensenada, Ensenada, Baja California, Mexico, [11]The Lyell Centre, Heriot Watt University, Edinburgh, UK, [12]Department of Earth Sciences, University of California, Santa Barbara, California, USA, [13]Department of Marine Sciences, University of Connecticut-Avery Point, Groton, Connecticut, USA, [14]MARUM-Center for Marine Environmental Sciences, University of Bremen, Bremen, Germany, [15]School of Earth and Atmospheric Sciences, Georgia Institute of Technology, Atlanta, Georgia, USA, [16]Alfred-Wegener Institute for Polar and Marine Sciences, Bremerhaven, Germany, [17]LSCE/IPSL, Laboratoire CNRS-CEA-UVSQ, Gif-sur-Yvette, France, [18]Department of Earth and Planetary Sciences, University of California, Davis, California, USA, [19]Max Planck Institute for Chemistry, Mainz, Germany, [20]Institute of Marine and Coastal Sciences, Rutgers University, New Brunswick, New Jersey, USA

Abstract The carbon isotope composition ($\delta^{13}C$) of seawater provides valuable insight on ocean circulation, air-sea exchange, the biological pump, and the global carbon cycle and is reflected by the $\delta^{13}C$ of foraminifera tests. Here more than 1700 $\delta^{13}C$ observations of the benthic foraminifera genus *Cibicides* from late Holocene sediments ($\delta^{13}C_{Cibnat}$) are compiled and compared with newly updated estimates of the natural (preindustrial) water column $\delta^{13}C$ of dissolved inorganic carbon ($\delta^{13}C_{DICnat}$) as part of the international Ocean Circulation and Carbon Cycling (OC3) project. Using selection criteria based on the spatial distance between samples, we find high correlation between $\delta^{13}C_{Cibnat}$ and $\delta^{13}C_{DICnat}$, confirming earlier work. Regression analyses indicate significant carbonate ion $(-2.6 \pm 0.4) \times 10^{-3}$‰/(μmol kg^{-1}) [$CO_3^{2-}$] and pressure $(-4.9 \pm 1.7) \times 10^{-5}$‰ m^{-1} (depth) effects, which we use to propose a new global calibration for predicting $\delta^{13}C_{DICnat}$ from $\delta^{13}C_{Cibnat}$. This calibration is shown to remove some systematic regional biases and decrease errors compared with the one-to-one relationship ($\delta^{13}C_{DICnat} = \delta^{13}C_{Cibnat}$). However, these effects and the error reductions are relatively small, which suggests that most conclusions from previous studies using a one-to-one relationship remain robust. The remaining standard error of the regression is generally $\sigma \cong 0.25$‰, with larger values found in the southeast Atlantic and Antarctic ($\sigma \cong 0.4$‰) and for species other than *Cibicides wuellerstorfi*. Discussion of species effects and possible sources of the remaining errors may aid future attempts to improve the use of the benthic $\delta^{13}C$ record.

1. Introduction

The stable carbon isotope composition ($\delta^{13}C$) measured in calcium carbonate shells (tests) of benthic foraminifera, particularly those of the genus *Cibicides* ($\delta^{13}C_{Cib}$), is one of the most widely used paleoceanographic tracers. Here we consider all benthic foraminifer species generally assumed to live epifaunally, e.g., of the genera *Cibicides* and *Cibicidoides*, a species of the genus *Cibicides*, for simplicity, because their classification is debated and has not reached consensus yet [e.g., *Schweizer et al.*, 2009]. $\delta^{13}C_{Cib}$ has been interpreted as evidence for changes in terrestrial carbon storage over glacial-interglacial time scales [*Peterson et al.*, 2014; *Shackleton*, 1977], changes in the efficiency of the biological pump [*Broecker*, 1982], and modulations of deep ocean nutrients and circulation [*Curry and Oppo*, 2005; *Duplessy et al.*, 1988; *Gebbie*, 2014; *Marchal and Curry*,

2008]. All of those interpretations assume that $\delta^{13}C_{Cib}$ reflects the $\delta^{13}C$ of dissolved inorganic carbon ($\delta^{13}C_{DIC}$) of bottom waters in a roughly one-to-one relationship as indicated by the pioneering, global-scale calibration of *Duplessy et al.* [1984, D84 thereafter]. This one-to-one relationship may be fortuitous since many other benthic foraminifer species show significant offsets with respect to bottom water $\delta^{13}C_{DIC}$ [*Corliss*, 1985; *Fontanier et al.*, 2006; *Ishimura et al.*, 2012; *McCorkle et al.*, 1990; *Rathburn et al.*, 1996]. The epibenthic (i.e., on or within the top ~1 cm of the sediment) habitat of *Cibicides* is advantageous compared to infaunal (abundance peak below the sediment surface) species because pore water conditions within the sediment differ from those of the bottom water due to organic matter respiration and mineral reactions [*Jorissen et al.*, 1995; *McCorkle et al.*, 1985; *Tachikawa and Elderfield*, 2002].

Despite the generally epibenthic habitat of *Cibicides*, different species within the genus are not all equivalent. Unfortunately, in the sediment one species appears when another vanishes, and hence, paired measurements and studies on the isotopic offsets between species are scarce. *Cibicides wuellerstorfi* (*C. wuellerstorfi*), also classified as *Cibicidoides wuellerstorfi*, *Planulina wuellerstorfi*, *Anomalina wuellerstorfi*, *Trancatulina wuellerstorfi*, and *Fontbotia wuellerstorfi*, is mostly reported as a one-to-one $\delta^{13}C_{DIC}$ recorder [*Belanger et al.*, 1981; *Zahn et al.*, 1986]. *Cibicides kullenbergi* (*C. kullenbergi* or *mundulus*) may yield lower $\delta^{13}C$ values than those of *C. wuellerstorfi* [*Gottschalk et al.*, 2016; *Hodell et al.*, 2001; *Martínez-Méndez et al.*, 2013], perhaps due to an occasional infaunal habitat of *C. kullenbergi*. Also for *Cibicides pachyderma* (*C. pachyderma*), $\delta^{13}C$ values lower than those of bottom water or of *C. wuellerstorfi* or *Planulina ariminensis* (*P. ariminensis*) have been reported suggesting that it may also live infaunally [*Fontanier et al.*, 2006; *Lynch-Stieglitz et al.*, 2014; *Mackensen and Licari*, 2004; *Schmiedl et al.*, 2004]. The $\delta^{13}C$ signature of *P. ariminensis*, which lives attached to elevated surfaces [*Lutze and Thiel*, 1989], has been reported as equivalent to that of *C. wuellerstorfi* [*Zahn et al.*, 1987]. *Mackensen and Licari* [2004] and *Murray* [2006] indicate lower $\delta^{13}C$ values for the genetically closely related species *Cibicides lobatulus* (*C. lobatulus*)[*Schweizer et al.*, 2009] than for *C. wuellerstorfi*, while *Weinelt et al.* [2001] report equivalent values for these two species. As a result, *C. wuellerstorfi* is the preferred species for paleoceanographic studies, but since it is not always present in the sediment, a vast number of data are often combined and reported as *C.* spp, perhaps given the difficulty of an unambiguous identification and/or low abundances of available (known) species. In any compilation of $\delta^{13}C_{Cib}$, interspecies differences are likely to contribute variability to the results. Here we attempt to update the general use of $\delta^{13}C_{Cib}$ as a paleoceanographic tracer, with an initial effort directed toward analysis of interspecies differences.

For their calibration D84 used $\delta^{13}C_{DIC}$ measurements from the Geochemical Ocean Sections Study (GEOSECS) cruise data sets collected during the 1970s [*Kroopnick*, 1985], which were much sparser and may have been less precise than measurements from more recent expeditions [*Schmittner et al.*, 2013]. D84 assembled 64 $\delta^{13}C_{Cib}$ data, but they did not report the criteria used to match the water column to the sediment data nor did they account for the effects of anthropogenic carbon. Moreover, the number of both sediment [*Peterson et al.*, 2014] and water column [*Schmittner et al.*, 2013] data has increased dramatically during the last 30 years, prompting a recalibration of the proxy, which is the primary focus of this paper. We attempt to improve the calibration compared to D84 not only by including more data but also by explicitly stating the selection criteria used to match the water column to the sediment data, by examining the sensitivity of the results to those choices, and by considering the effects of anthropogenic carbon.

Other important goals are the quantification of deviations in the $\delta^{13}C_{DIC}$-$\delta^{13}C_{Cib}$ relationship, and the evaluation of any contribution to these deviations from secondary effects of carbonate ion concentration [CO_3^{2-}], temperature, and pressure. Laboratory culture studies of planktic foraminifera show that shell calcite $\delta^{13}C$ values decrease by 0.006 to 0.015‰/(μmol kg^{-1}) increase of the sea water [CO_3^{2-}] concentration at constant $\delta^{13}C_{DIC}$ [*Spero et al.*, 1997]. Although such studies have not yet been conducted on benthic foraminifera because they are difficult to grow in the laboratory [*Wollenburg et al.*, 2015], observations of modern individual foraminifera suggest that benthics are also affected [*Ishimura et al.*, 2012], which could significantly impact reconstructions of past $\delta^{13}C_{DIC}$. Recent theoretical work using diffusion-reaction modeling of carbon isotopes in single foraminifera not only confirms the postulated carbonate ion effect but also indicates significant temperature and pressure effects on isotopic fractionation between surrounding bottom waters and benthic foraminiferal shells [*Hesse et al.*, 2014].

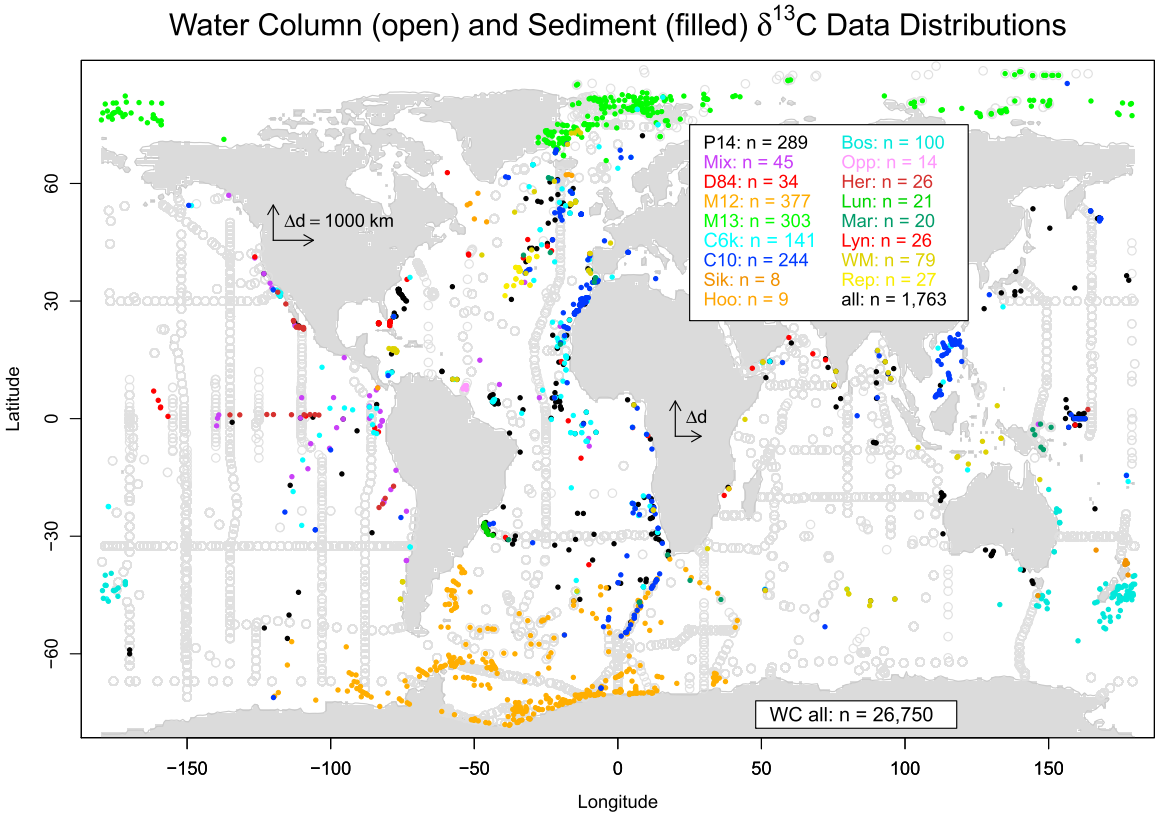

Figure 1. Map of water column $\delta^{13}C_{DIC}$ (open light grey circles) and core top benthic foraminifera $\delta^{13}C_{cib}$ (filled circles) data distributions. Arrows over North America and Africa are scale distances Δd of 1000 km, which we use as a selection criterion to compare the two data sets. The sediment data set includes a total of 1763 data points from the epibenthic foraminifera genus *Cibicides*, derived from merging 17 data sets (see Table 1 and text for details).

In addition, *Mackensen et al.* [2001, 1993] suggest that $\delta^{13}C_{Cib}$ may underestimate bottom water $\delta^{13}C_{DIC}$ if the foraminifera live on sediments that receive pulses of phytodetritus, the decomposition of which would lower the calcifying microenvironment $\delta^{13}C_{DIC}$ with respect to that of the overlaying bottom water. This is of particular concern in the Southern Ocean, where large spatial gradients in glacial $\delta^{13}C_{Cib}$ have been observed [*Hodell et al.*, 2003; *Lund et al.*, 2015; *Waelbroeck et al.*, 2011].

We present the initial core top calibration of OC3, an international working group of the Past Global Changes (PAGES) program, which has the broader goal of compiling benthic carbon isotope data and estimating their uncertainties in order to reconstruct past changes in ocean circulation and carbon cycling (http://www.past-globalchanges.org/index.php/ini/wg/oc3/intro). We expect that the database and calibration will be updated in the future. Sediment and water column data are available at the National Oceanographic and Atmospheric Administration's National Centers for Environmental Information (Paleoclimate; https://www.ncdc.noaa.gov/paleo-search/study/21750).

2. Methods

The locations of our updated compilations of water column and surface sediment data are shown in Figure 1.

2.1. Water Column Data

Our new compilation is based on 18,587 measurements including WOCE and CLIVAR (Climate and Ocean: Variability, Predictability and Change) cruises from years 1990 to 2005 [*Schmittner et al.*, 2013; S13 thereafter]. One duplicate cruise (58AA20010527_ATL) was removed from the original S13 data set (see Acknowledgements). To this data set, we added 1486 data from the PACIFICA database (http://cdiac3.ornl.gov/waves/discrete/ accessed 28 November 2013) of two North Pacific cruises (cruisenumbers/expocodes: 318 M200406/318 M20040615, 49MR01K04_1/49NZ20010723) from 2001 and 2004. We also included 2248

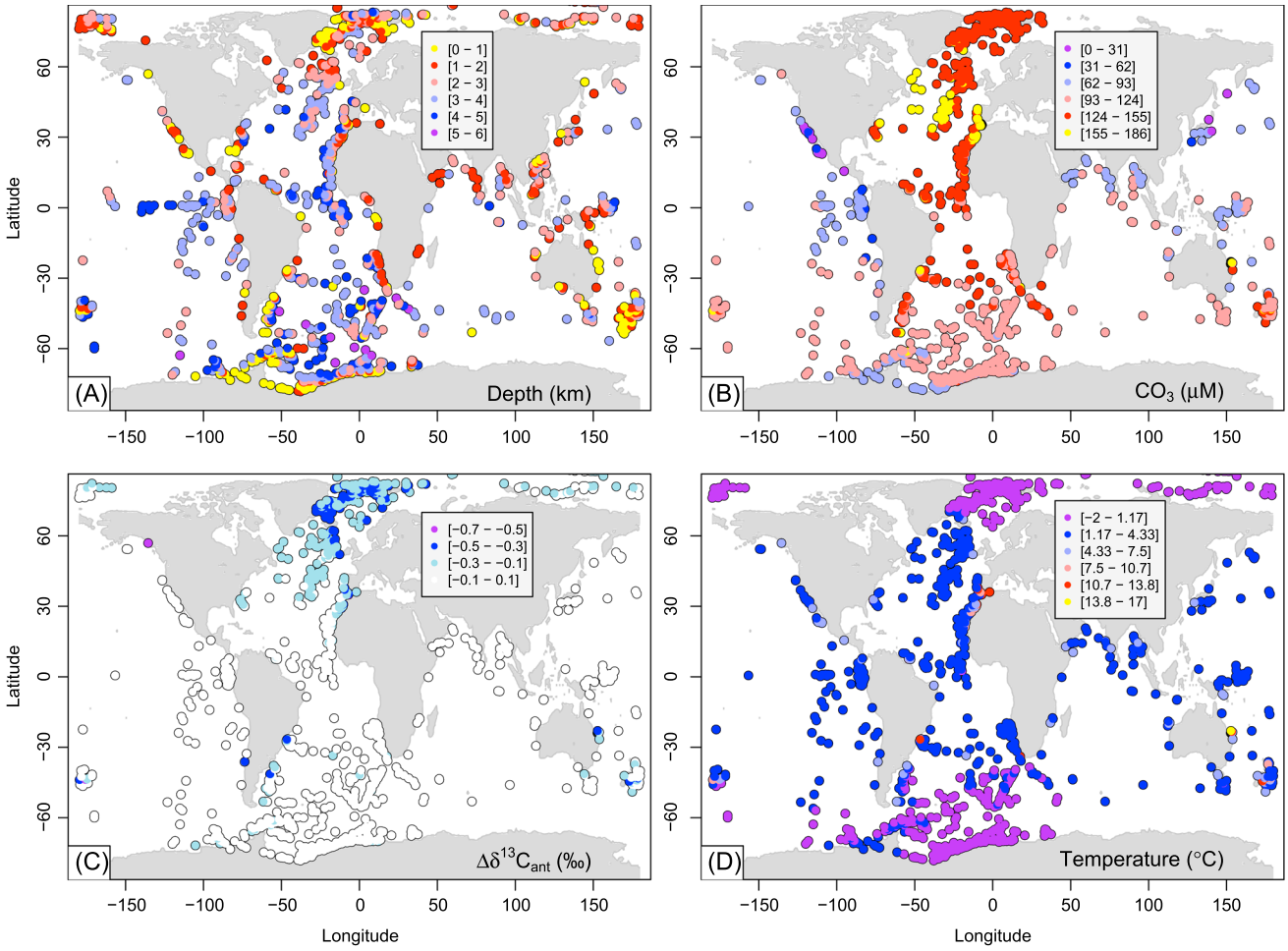

Figure 2. Maps of (a) water depth, (b) observed carbonate ion concentration, (c) modeled anthropogenic $\delta^{13}C$ correction ($\Delta\delta^{13}C_{ant}$), and (d) observed temperature. Criteria of Δd = 1000 km, $\Delta z = z/5$ were used to map water column observations and model results.

data from the earlier GEOSECS campaign (extracted from Ocean Data View on 21 September 2007) [*Kroopnick*, 1985], 639 observations from two recent GEOTRACES cruises, GI04 (205 data from the Indian Ocean from year 2009) and GA03 (434 measurements from the North Atlantic from years 2010–2011) [*Quay and Wu*, 2015], 3339 data from the Atlantic and Indian Ocean sectors of the Southern Ocean from 1989 to 2003 [*Mackensen*, 2012; M12 thereafter], 274 data from Arctic bottom waters from years 1990 to 2008 [*Mackensen*, 2013; M13 thereafter], and 68 data from the southeastern margin of the Pacific [*Martínez-Méndez et al.*, 2013]. The following 110 new (unpublished) measurements by Gema Martínez-Méndez were added as well: 60 data from the tropical West Pacific (Papua New Guinea: 14, Mindanao: 46), 9 data from the southeast Pacific, 24 data from the subtropical northeast Atlantic, and 17 from the subtropical South Atlantic. From the original M12 and M13 data sets 133 and 2 data were removed, respectively, because they included negative outliers, which were determined subjectively by inspecting individual and multiple neighboring vertical profiles. Such outliers, which have been reported since the early measurements of *Kroopnick* [1985], may be caused by contamination of the water samples. From the original M13 data set we have also removed five data from the ODEN cruise and four data from the GEOSECS cruises because they are already included. In total the updated data set consists of 26,750 individual observations, with broad spatial coverage, although large gaps remain in some regions such as the eastern equatorial Atlantic, the South China Sea, and adjacent parts of the western tropical Pacific, and the Indian and western Pacific sectors of the Southern Ocean (Figure 1). The S13 data set also includes dissolved inorganic carbon (DIC) and alkalinity (ALK) observations, from which carbonate ion concentrations

Table 1. Data Sets Used[a]

	N	Time	Species	References and Comments	Contributor
				Late Holocene Fossil Data	
P14	289	0–6 ka	*C. spp**	Global compilation from *Peterson et al.* [2014]	C. Peterson
Mix	45	uH	*C. wue*	Unpublished global compilation	A. C. Mix
D84	34	uH	*C. spp**, *C. wue*	*Duplessy et al.* [1984] global data with duplicates with P14 removed	
C6k	141	0–6 ka	*Cibs.*	Global	O. Cartapanis
C10	244	uH	*Cibs.*	Global, top 10 cm, $\delta^{18}O$ checked	O. Cartapanis
Bos	100	0–7 ka	*C. wue*, *C. spp*	Southwest Pacific compilation partly described in *Cortese and Prebble* [2015] and *Prebble et al.* [2013] including unpublished data	H. Bostock
Opp	14	0–5 ka	*C. wue*, *C. pac*	Unpublished data from the Demerara Rise around 8°N in the western Atlantic	D. Oppo
Her	26	uH	*P. wue*	Pacific (Baja California, equatorial Pacific Nazca Ridge) data set partly described in *Herguera et al.* [2010]	J. C. Herguera
Lun	21	0.9–6.4 ka	*C. wue*, *C. flo*	Brazil Margin compilation from *Lund et al.*, 2015 and unpublished data from the Florida Straits	D. Lund
Mar	20	uH	*C. wue*, *C. spp*	Published data from the South and northwest Atlantic, and six new measurements from the equatorial West Pacific	G. Marnínez-Méndez
Lyn	26	0–6 ka uH	*P. wue, C. pac, C. spp, P. ari*	Unpublished data from the tropical Pacific and Florida Straits	J. Lynch-Stieglitz
WM	79	0–4 ka 0–2 ka	*C. wue*, *C. spp*, *C. kul*, *C. pac*, *C. bra*, *C. psu*	Global compilation of published and unpublished data	C. Waelbroeck and E. Michel
Sik	8	0–6 ka	*C. wue*, *C. spp*	Unpublished data from the southwest Pacific	E. Sikes
Hoo	9	0–5 ka	*C. wue*, *C. lob*	Mostly North Atlantic data including those described in *Hoogakker et al.* [2011] and one datapoint from the equatorial Pacific	B. Hoogakker
Rep	27	uH	*C. wue*	Data from cruise MSM58 along the Mid Atlantic Ridge 42.47°N to 31.37°N	J. Repschläger
				Modern (Mostly Living) Foraminifera	
M12	377	0 ka	*C. spp**	Southern Ocean data from *Mackensen* [2012]	A. Mackensen
M13	303	0 ka	*C. spp**	Arctic data from *Mackensen* [2013]	A. Mackensen
All	**1763**				

[a]The left row indicates the abbreviated name used throughout the paper. N denotes the number of data. Time constraints include "upper Holocene" (uH), which was determined from $\delta^{18}O$ and the upper 10 cm of sediment (C10), which was also checked for $\delta^{18}O$. Species information is available for some data sets. However, for those indicated as *C. spp** species information is not available for individual data but the general information is available in the text. *Cibs.* Refers to various *Cibicides* species with detailed information available in the data spreadsheet. Species abbreviations are *C. wuellerstorfi* (*C. wue*), *C. kullenbergi* (*C. kul*), *C. pachyderma* (*C. pac*), *C. lobatulus* (*C. lob*), *P. ariminensis* (*P. ari*), *C. floridanus* (*C. flo*).

were approximated using the relationship $[CO_3^{2-}] \cong$ ALK-DIC [*Zeebe and Wolf-Gladrow,* 2001], as well as measurements of temperature (Figure 2d) and other variables. In case in situ $[CO_3^{2-}]$ or temperature was not available we filled in climatological values from the Global Data Analysis Project [*Key et al.*, 2004] and World Ocean Atlas 2005 [*Locarnini et al.*, 2006].

Note that although not very well documented, $\delta^{13}C_{DIC}$ likely varies on seasonal to multicentennial and longer timescales. Therefore, the water column $\delta^{13}C_{DIC}$ data represent mostly snapshots in time of a temporally and spatially varying field. Generally, we can expect the temporal variations to be larger near the surface than in the deep ocean. Temporal variability of $\delta^{13}C_{DIC}$ will therefore be a possible reason for offsets with the sediment data.

2.2. Surface Sediment Data

For our new compilation of foraminiferal measurements two types of data are included (Table 1 and Figure 1).

1. Sediment core top measurements of fossil foraminifera shells represent a long-term average covering the Late Holocene (LH; approximately the last 6000 years). The 1083 data from 15 data sets have been assembled. Efforts to remove duplicates with already existing data were undertaken by manually sorting with respect to depth and subsequent visual inspection of nearby entries with identical or similar latitude, longitude, and core name. Duplicates are excluded in the counts in Table 1. Many data sets do not provide species information for individual data. For instance, P14 included records which the original authors described as "*Cibs* equivalent," or "in equilibrium with $\delta^{13}C_{DIC}$," but records listed as "mixed benthics" were not included. Species information is currently available for a subset of 642 data, of which 550 are *C. wuellerstorfi*, 37 are *C. kullenbergi*, 12 are *C. lobatulus*, 34 are *C. pachyderma*, and 9 are *C. floridanus*.

Despite this limited amount of information, we provide an initial analysis of species dependence. Size information is not always available either.

2. Measurements on modern, mostly living foraminifera, represent contemporary conditions but are limited to high latitudes. Southern Ocean measurements cover years 1983 to 2001 (M12), and Arctic observations are from 1987 to 2012 (M13). Each data point represents typically three shells, which is similar to downcore data, although the LH data may represent a larger number of shells since many of them were averaged over the last ~6 ka. M12 and M13 data sets are exclusively based on surface sediment samples taken by large box or multiple corer. M12 and M13 used preferentially *C. wuellerstorfi*, and, where not available, *Cibicides refulgens* and *C. lobatulus*. In M12 also *C. pachyderma*, *C. kullenbergi*, and *P. ariminensis* are included.

The total number of data is 1763, approximately 28-fold more data than considered by D84. The sediment data span depths ranging from 64 m to 5691 m and all ocean basins (Figure 2a).

Note that the averaging period of the different data sets is different. The measurements on "living" foraminifera represent a short, essentially instantaneous snapshot of the modern ocean. "Living" foraminifera are defined as those stained by rose Bengal, but see, for instance, *Bernhard et al.* [2006] regarding vitality assessments of foraminifera using rose Bengal. In contrast, the LH core top data represent a heterogeneous assemblage of long-term averages likely covering thousands of years (ka). P14, C6k, and Lyn use the last 6 ka, Bos uses the last 7 ka, and C10 uses the upper 10 cm of the sediment, whereas the averaging period for Mix, Rep, and D84 is simply defined as "upper Holocene" (uH) as determined from oxygen isotope values from the same samples. Oxygen isotopes from the C10 data have been checked to make sure they represent late Holocene conditions. Brazil Margin results (Lun), based on the uppermost sediment in each of the cores, which were radiocarbon dated between 900 to 6400 years BP, were preferred over longer time averages of the same cores included in any of the other data sets. Many of the core top samples analyzed are not precisely dated. Some (in piston cores) may be contaminated by older material brought up by piston effects, or by overpenetration leading to the loss of the sediment water interface in the coring process. Data from multicores that preserve pristine sediment-water interfaces are preferable and should be identified and compared to those from piston cores in future work. A limited, local comparison from the Florida Straits indicates no systematic offsets, but differences of 0.1–0.2‰ between multicore and piston cores. For most sites, however, information on the coring equipment is not yet available in our database. Surface sediment data from box and multicores can also be contaminated by older sedimentary material at sites affected by erosion or winnowing. The only ways to exclude older material is via radiometric dating of the samples or comparison of foraminifera oxygen isotope values with nearby cores.

2.3. Mapping Procedure

Water column and sediment data are generally not colocated. In order to map the water column data to the sediment data, we use the horizontal great-circle distance (Δd) and the vertical distance (Δz) from the locations (longitude, latitude, and depth) of the sediment data as a criterion. All water column data within those distances are averaged with equal weighting. Results are presented for two different choices: a more liberal one (Δd = 1000 km, indicated in Figure 1, $\Delta z = z/5$), which will be the default, and a more conservative one (Δd = 500 km, $\Delta z = z/10$). The depth dependence for the vertical distance is motivated by the fact that like most other ocean tracer distributions, $\delta^{13}C_{DIC}$ shows larger vertical gradients in the upper ocean than in the deep [*Schmittner et al.*, 2013]. It leads to layer thicknesses of Δz = 100 m and 1 km at depths of z = 500 m and 5 km, respectively, for the more liberal criterion and 50 m and 500 m, respectively, for the more conservative criterion. Mapped water column carbonate ion concentrations and temperatures are shown in Figure 2.

2.4. Anthropogenic Carbon

The invasion of ^{13}C-depleted carbon into the upper ocean during the past century [*Böhm et al.*, 2002] from the burning of fossil fuels has decreased $\delta^{13}C_{DIC}$ in the upper ocean during the past decades, a process known as the Suess Effect [*Gruber et al.*, 1999; *Keeling*, 1979; *Suess*, 1955]. Thus, some water column and modern foraminiferal data have reduced $\delta^{13}C$ values due to anthropogenic $\delta^{13}C_{DIC}$ ($\Delta\delta^{13}C_{ant}$). The magnitude of the offset varies depending on location and year the cores were collected. Hence, the Suess effect could bias some comparisons to LH sediment data.

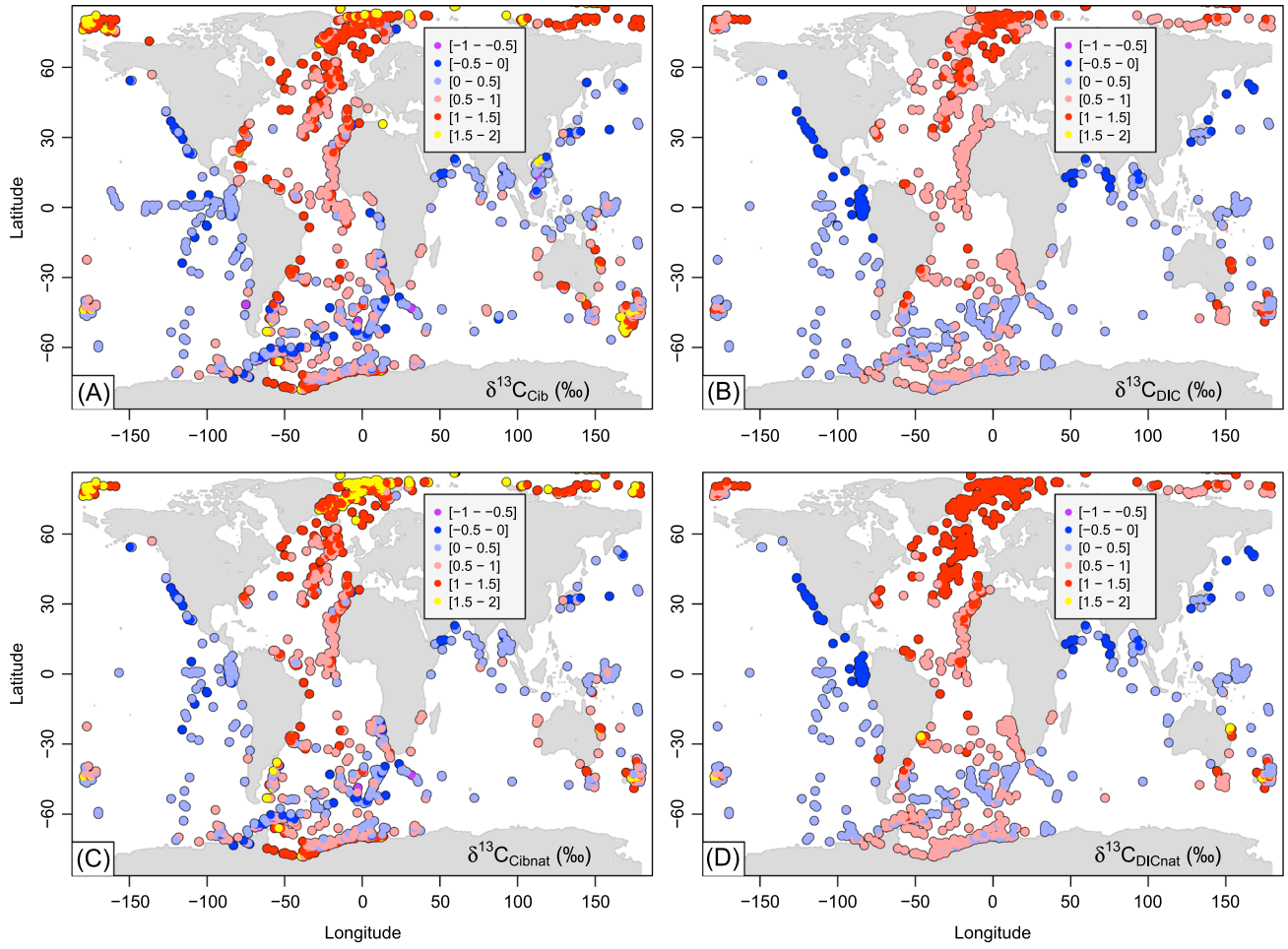

Figure 3. Maps of sediment core top (a and c, $\delta^{13}C_{Cib}$) and mapped water column (b and d, $\delta^{13}C_{DIC}$) distributions. Figures 3a and 3b show the raw data, which include anthropogenic effects. Figures 3c and 3d display estimates of natural (preindustrial) $\delta^{13}C$ distributions calculated by subtracting model simulated anthropogenic $\Delta\delta^{13}C_{ant}$ (Figure 2c). Liberal selection criteria (Δd = 1000 km, $\Delta z = z/5$) were used in all panels.

Here we use model-based estimates of $\Delta\delta^{13}C_{ant}$ from *S*13's "FeL" (iron limitation) simulation, which were subtracted from the water column data and from the M12 and M13 sediment data to yield estimates of natural (preindustrial) $\delta^{13}C_{DICnat} = \delta^{13}C_{DIC} - \Delta\delta^{13}C_{ant}$ and $\delta^{13}C_{Cibnat} = \delta^{13}C_{Cib} - \Delta\delta^{13}C_{ant}$. Note that we did not subtract $\Delta\delta^{13}C_{ant}$ from the LH sediment data since we assume they are unaffected by the Suess effect. The model results were interpolated and extrapolated onto the locations of the observations. We account for the time dependency of the anthropogenic signal by using decadal averages from the 1970s to the 2000s separately, depending on the decade the measurements were taken. This method only yields magnitudes of $\Delta\delta^{13}C_{ant}$ that exceed −0.1‰ in the northern North Atlantic, the Nordic Seas, and a few shallow cores elsewhere (Figure 2c).

3. Results

In this section the water column data are first compared to the sediment data directly. Then results of multiple regression analyses are presented considering $[CO_3^{2-}]$ and pressure effects. In addition to the results shown in the remainder of the main text we have conducted a regional analysis, which is presented in the accompanying supporting information (SI). Note also that water column data are not available at each of the sediment core locations given the spatial matching criteria, which reduces the number of data pairs *n* that can be used for comparison. For the liberal mapping criterion only 1492 out of the total of 1763 sediment data are mapped with water column data (e.g., Figures 3a versus 3b). For instance, in the tropical Pacific

Table 2. Parameters of the Linear Regression Analyses Equation (1)[a]

E	*n*	r^2	σ (‰)	*a* (‰)	*b*	*c* (10^{-3}‰/μM)	*d* (10^{-5}‰/m)
LA1	**1402**	**0.12**	**0.29**	**0.45 ± 0.03**	**1**	**−2.2 ± 0.2**	**−6.6 ± 0.6**
LA2		|0.12|	|0.29|	|0.35 ± 0.03|	|1|	|−0.6 ± 0.2*|	|−8.3 ± 0.6|
LA3		0.05	0.30	0.29 ± 0.03	1	−2.2 ± 0.3	0
LA4		0.07	0.30	0.18 ± 0.02	1	0	−6.6 ± 0.6
LA5		NA	0.31	0	1	0	0
LA6		0.65	0.31	0.11 ± 0.02	0.89 ± 0.02	0	0
LA7		|0.57|	|0.31|	|0.13 ± 0.02|	|0.94 ± 0.02|	|0|	|0|
LL1	**835**	**0.18**	**0.25**	**0.41 ± 0.03**	**1**	**−2.7 ± 0.2**	**−4.4 ± 0.8**
LL2		|0.18|	|0.25|	|0.41 ± 0.03|	|1|	|−0.7 ± 0.2|	|−10.0 ± 0.8|
LL3		0.15	0.25	0.31 ± 0.03	1	−3.0 ± 0.02	0
LL4		0.04	0.27	0.11 ± 0.02	1	0	−4.9 ± 0.9
LL5		NA	0.27	0	1	0	0
LL6		0.71	0.25	0.13 ± 0.01	0.78 ± 0.02	0	0
LL7		|0.65|	|0.27|	|0.15 ± 0.02|	|0.88 ± 0.02|	0	0
LW1	**412**	**0.25**	**0.21**	**0.48 ± 0.04**	**1**	**−2.8 ± 0.3**	**−5.0 ± 1.1**
LW5		NA	0.25	0	1	0	0
LW6		0.78	0.22	0.17 ± 0.02	0.77 ± 0.02	0	0
CA1	**907**	**0.15**	**0.29**	**0.49 ± 0.04**	**1**	**−2.4 ± 0.3**	**−7.1 ± 0.8**
CA2		|0.16|	|0.29|	|0.42 ± 0.04|	|1|	|−1.0 ± 0.3|	|−9.3 ± 0.8|
CA3		0.07	0.31	0.35 ± 0.04	1	−2.7 ± 0.3	0
CA4		0.10	0.30	0.23 ± 0.02	1	0	−7.7 ± 0.8
CA5		NA	0.32	0	1	0	0
CA6		0.60	0.31	0.14 ± 0.02	0.86 ± 0.02	0	0
CA7		|0.53|	|0.31|	|0.14 ± 0.02|	|0.90 ± 0.03|	0	0
CL1	**501**	**0.19**	**0.25**	**0.41 ± 0.04**	**1**	**−2.8 ± 0.3**	**−3.8 ± 1.0**
CL2		|0.21|	|0.25|	|0.46 ± 0.04|	|1|	|-1.0 ± 0.3|	|−10.4 ± 1.0|
CL3		0.17	0.26	0.34 ± 0.04	1	−3.0 ± 0.3	0
CL4		0.05	0.27	0.14 ± 0.03	1	0	−5.5 ± 1.1
CL5		NA	0.28	0	1	0	0
CL6		0.69	0.25	0.14 ± 0.02	0.76 ± 0.02	0	0
CL7		|0.65|	|0.27|	|0.16 ± 0.02|	|0.84 ± 0.03|	0	0
CW1	**247**	**0.25**	**0.22**	**0.44 ± 0.05**	**1**	**−2.9 ± 0.4**	**−3.1 ± 1.4**
CW5		NA	0.27	0	1	0	0
CW6		0.76	0.22	0.19 ± 0.02	0.74 ± 0.03	0	0

[a]E: experiment name. The first letter of the experiment name indicates the selection criterion: L = liberal, C = conservative. The second letter denotes whether All (A), only LH (L), or only *C. wuellerstorfi* (W) data have been used. Each set of experiments separated by a horizontal line uses the same data. N: number of data, r^2: squared correlation coefficient, σ: residual standard error, *a*: intercept, *b*–*d*: slopes. Asterisks (*) denote values not significantly different from zero at the 0.01 significance level using a student's *t* test. Results in vertical bars || include anthropogenic $\delta^{13}C_{DIC}$ for comparison with the lines directly above.

around 140°W no water column data are available at the depth of the sediment data and within the horizontal distance criterion. Similarly, in the eastern tropical Atlantic no water column data are available for comparison to the foraminifera data. Thus, our comparison is not only limited by the number of sediment data but also by the sparse coverage of water column data. The amount of data available for the multiple linear regressions presented below is further reduced due to the limited availability of [CO_3^{2-}] data such that for model LA1 in Table 2, only 1402 triplets of $\delta^{13}C_{Cibnat}$, $\delta^{13}C_{DICnat}$, and [CO_3^{2-}] exist. For the conservative mapping criteron these numbers are further reduced (see Tables 2 and 3).

3.1. Spatial Distributions of Sedimentary and Water Column Carbon Isotopes

The raw core top $\delta^{13}C_{Cib}$ data vary from values of more than 1.9‰ in the Arctic and a few shallow cores from elsewhere to less than −0.7‰ in the Atlantic sector of the Southern Ocean (Figure 3a). Atlantic values are mostly greater than 0.5‰, whereas in the Indian and Pacific Ocean they are mostly below 0.5‰, except for some of the shallower sites. The water column $\delta^{13}C_{DIC}$ values mapped onto the sediment data display similar interbasin differences, but the variations are much smoother (Figure 3b). Maximum values do not

Table 3. Standard Deviations (σ) and Biases ($-\bar{\varepsilon}$) for Individual Data Sets and Species, and Four Experiments (LA1, CA1, LA5, and CA5) as Listed in Table 2[a]

	LA1			CA1			LA5			CA5		
	σ (‰)	$-\bar{\varepsilon}$ (‰)	n	σ (‰)	$-\bar{\varepsilon}$ (‰)	n	σ (‰)	$-\bar{\varepsilon}$ (‰)	n	σ (‰)	$-\bar{\varepsilon}$ (‰)	n
All	0.29	0.00	1402	0.29	0.00	907	0.33	0.05	1492	0.33	0.07	1097
						Data Sets						
P14	0.24	0.00	250	0.24	0.01	158	0.27	0.01	250	0.27	0.02	158
Mix	**0.22**	**0.05**	34	**0.24**	**0.05**	25	**0.32**	**0.17**	34	**0.34**	**0.19**	25
D84	0.18	0.01	30	0.21	−0.07	16	0.19	0.02	30	0.20	0.01	16
M12	**0.39**	0.04	369	**0.35**	0.03	331	**0.42**	0.11	375	**0.39**	0.11	331
M13	0.25	**0.07**	198	0.20	**0.04**	69	0.34	**0.20**	277	0.20	**0.08**	69
C6k	0.22	−0.05	121	0.22	−0.05	85	0.24	−0.07	124	0.23	−0.08	85
C10	**0.32**	−0.10	179	**0.33**	−0.08	108	**0.33**	−0.10	180	**0.34**	−0.07	108
Bos	0.25	−0.04	75	0.30	−0.13	29	0.25	0.01	75	0.31	−0.08	29
Opp	0.26	−0.05	14	0.16	0.12	7	0.18	−0.01	14	0.10	0.07	7
Her	**0.20**	**−0.01**	19	**0.20**	**−0.06**	15	**0.25**	**0.21**	19	**0.25**	**0.23**	15
Lun	0.20	0.11	12	0.18	0.13	12	0.21	0.12	12	0.20	0.14	12
Mar	0.17	0.09	20	0.22	0.07	16	0.20	0.11	20	0.22	0.12	16
Lyn	0.06	0.06	1	–	–	0	0.09	0.09	1	–	–	0
WM	0.23	−0.11	47	0.21	−0.08	23	0.26	−0.10	48	0.26	−0.06	23
Sik	0.12	0.05	8	0.14	0.04	7	0.16	0.12	8	0.20	0.51	1
Hoo	0.28	0.04	9	0.27	−0.07	6	0.33	0.01	9	0.32	−0.13	6
Rep	0.16	−0.03	16	–	–	0	0.19	−0.12	16	–	–	0
						Species						
Wue	0.21	0.01	413	0.23	0.00	247	0.25	0.02	415	0.27	0.03	258
Kul	0.35	−0.15	31	0.23	−0.08	13	0.36	−0.16	32	0.31	−0.04	15
Lob	0.57	−0.47	12	0.47	−0.37	5	0.50	−0.39	12	0.36	−0.23	8
Pac	0.30	−0.24	11	0.26	−0.16	3	0.20	−0.12	11	0.20	−0.12	3

[a]However, here for LA5 and CA5 we use all mapped data in contrast to the results presented in Table 2, which used a slightly smaller data set for which also $[CO_3^{2-}]$ data were available. Highlighted in bold are some features discussed in the text such as larger errors of M12 and C10 and reduction of the positive biases for the Pacific (Her and Mix) and Arctic (M13) data for LA1 and CA1 models compared with LA5 and CA5, respectively. Species are *C. wuellerstorfi* (Wue), *C. kullenbergi* (Kul), *C. lobatulus* (Lob), and *C. pac* (Pac).

exceed 1.4‰, about 0.6‰ lower than those of the highest $\delta^{13}C_{Cib}$ data. The lowest values of $\delta^{13}C_{DIC}$ (−0.5‰) occur in the northern Indian and Pacific Oceans between about 1 and 2 km depth whereas the $\delta^{13}C_{Cib}$ minima are found in the South Atlantic, where bottom water $\delta^{13}C_{DIC}$ is generally above 0‰. The standard deviation of the sediment data of $\sigma(\delta^{13}C_{Cib})$ = 0.48‰ is higher than that of the water column data $\sigma(\delta^{13}C_{DIC})$ = 0.38‰.

Our estimates of $\delta^{13}C_{Cibnat}$ (Figure 3c) are similar to the $\delta^{13}C_{Cib}$ data except in the Arctic and subarctic North Atlantic and at a few shallow cores elsewhere, where the model predicts a substantial Suess effect (Figure 2c). Consequently, the water column $\delta^{13}C_{DICnat}$ estimates (Figure 3d) are higher than the $\delta^{13}C_{DIC}$ data in those regions. However, $\delta^{13}C_{DIC}$ data are affected by anthropogenic carbon in the deep midlatitude North Atlantic as far south as the subtropics, where most $\delta^{13}C_{DICnat}$ values are above 1‰. In contrast, not much difference is seen between $\delta^{13}C_{Cibnat}$ and $\delta^{13}C_{Cib}$ there as a consequence of our assumption that the LH data do not need to be corrected for anthropogenic effects. These results are consistent with observational estimates of intense uptake of anthropogenic carbon by deep water formation in the North Atlantic [*Khatiwala et al.*, 2009; *Olsen and Ninnemann*, 2010]. Consistent with previous results [*Schmittner et al.*, 2013], the standard deviations of the preindustrial $\sigma(\delta^{13}C_{Cibnat})$ = 0.53‰ and $\sigma(\delta^{13}C_{DICnat})$ = 0.47‰ are higher than those of the contemporary data, and, again, the sediment data have a larger standard deviation than the water column data, which indicates that $\delta^{13}C_{Cib}$ is influenced by additional processes than $\delta^{13}C_{DIC}$.

The $\delta^{13}C_{DICnat}$ estimates in the deep ocean (~1500 to 3500 m) decrease along the flow path of deep water from the North Atlantic south into the Southern Ocean and northward from the Southern Ocean into the Indian and Pacific oceans (Figures 4c and 4d). Along its path, water accumulates ^{13}C-depleted carbon from the sinking and remineralization of organic matter which is the most important effect explaining the gradual decrease in deep water $\delta^{13}C_{DICnat}$ from the Atlantic to the Pacific [*Kroopnick*, 1985; *Schmittner et al.*, 2013]. In

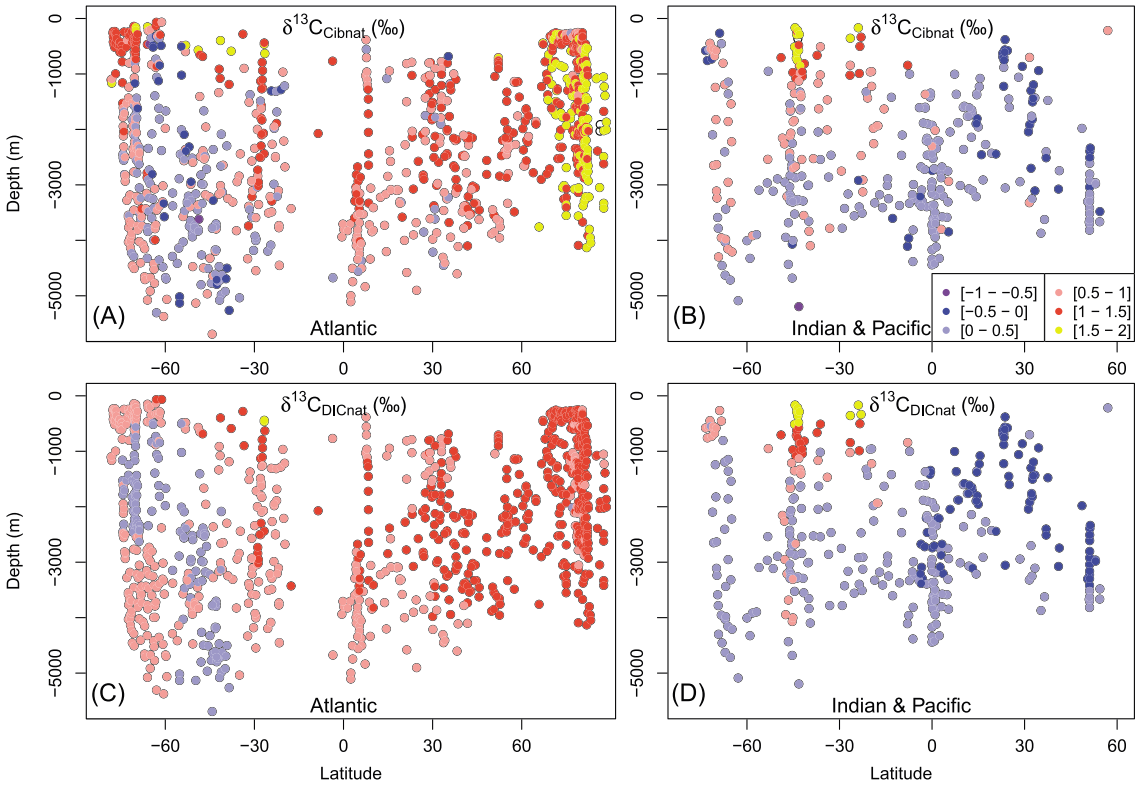

Figure 4. Latitude-depth sections from the (a and c) Atlantic and (b and d) Pacific for $\delta^{13}C_{Cibnat}$ (Figures 4a and 4d) and $\delta^{13}C_{DICnat}$ (Figures 4c and 4d). Liberal selection criteria (Δd = 1000 km, $\Delta z = z/5$) were used in all panels.

the South Atlantic a local minimum of $\delta^{13}C_{DICnat} < 0.5‰$ extends in a belt which runs east-northeast from the Drake Passage to the southern tip of Africa (Figure 3d), while deepening from ~1 km south of 60°S to ~5 km around 45°S (Figure 4c). This region of relatively old and respired carbon-rich Circumpolar Deep Water from the Pacific separates higher $\delta^{13}C_{DICnat}$ values in North Atlantic Deep Water to the north from higher values of Weddell Sea Bottom Water to the south (Figure 3d). Elevated $\delta^{13}C_{DIC}$ values of Weddell Sea Bottom Water have been attributed to the imprint of thermodynamic fractionation during air-sea gas exchange [*Charles and Fairbanks*, 1990; *Mackensen*, 2012].

Differences between contemporary sediment and water column data ($\Delta = \delta^{13}C_{Cib} - \delta^{13}C_{DIC}$) range mostly within ±0.7‰, although larger differences occur at some individual locations particularly at high latitudes (Figures 5a and 6a and 6b). The arithmetic mean of $\delta^{13}C_{Cib}$, $\overline{\delta^{13}C}_{Cib} = 0.76‰$ is about 0.12‰ higher than the water column value $\left(\overline{\delta^{13}C}_{DIC} = 0.64‰\right)$. Removing the effect of anthropogenic carbon impacts the differences mainly in the North Atlantic, where it leads to higher $\delta^{13}C_{DICnat}$ compared to $\delta^{13}C_{DIC}$. This shifts most sediment data there from being higher to being lower than the water column data (Figure 5b). The mean values increase to $\overline{\delta^{13}C}_{Cibnat} = 0.82‰$ and $\overline{\delta^{13}C}_{DICnat} = 0.76‰$, but a substantial and statistically highly significant difference (0.07‰, $p < 0.0001$ using a two-sided t test) remains.

The standard deviation of the difference $\sigma_{\Delta nat}$ can be interpreted as an error estimate of carbon isotope reconstructions assuming a one-to-one relationship between $\delta^{13}C_{Cibnat}$ and $\delta^{13}C_{DICnat}$. Using the data from Figure 5c yields $\sigma_{\Delta nat}$ = 0.33‰, which is more than twice as large as that reported by D84. However, as we will show below, our estimate is inflated by inclusion of data from living foraminifera (M12) from the Southern Ocean, which are noisier than most other sediment data.

Water column measurements have their own errors. We estimate the $\delta^{13}C_{DICnat}$ error by calculating the standard deviation σ_{DICnat} of the water column data that contribute to the average at each sediment core location. Whereas most values of σ_{DICnat} are below 0.2‰, at high latitudes values of 0.3‰ are frequent

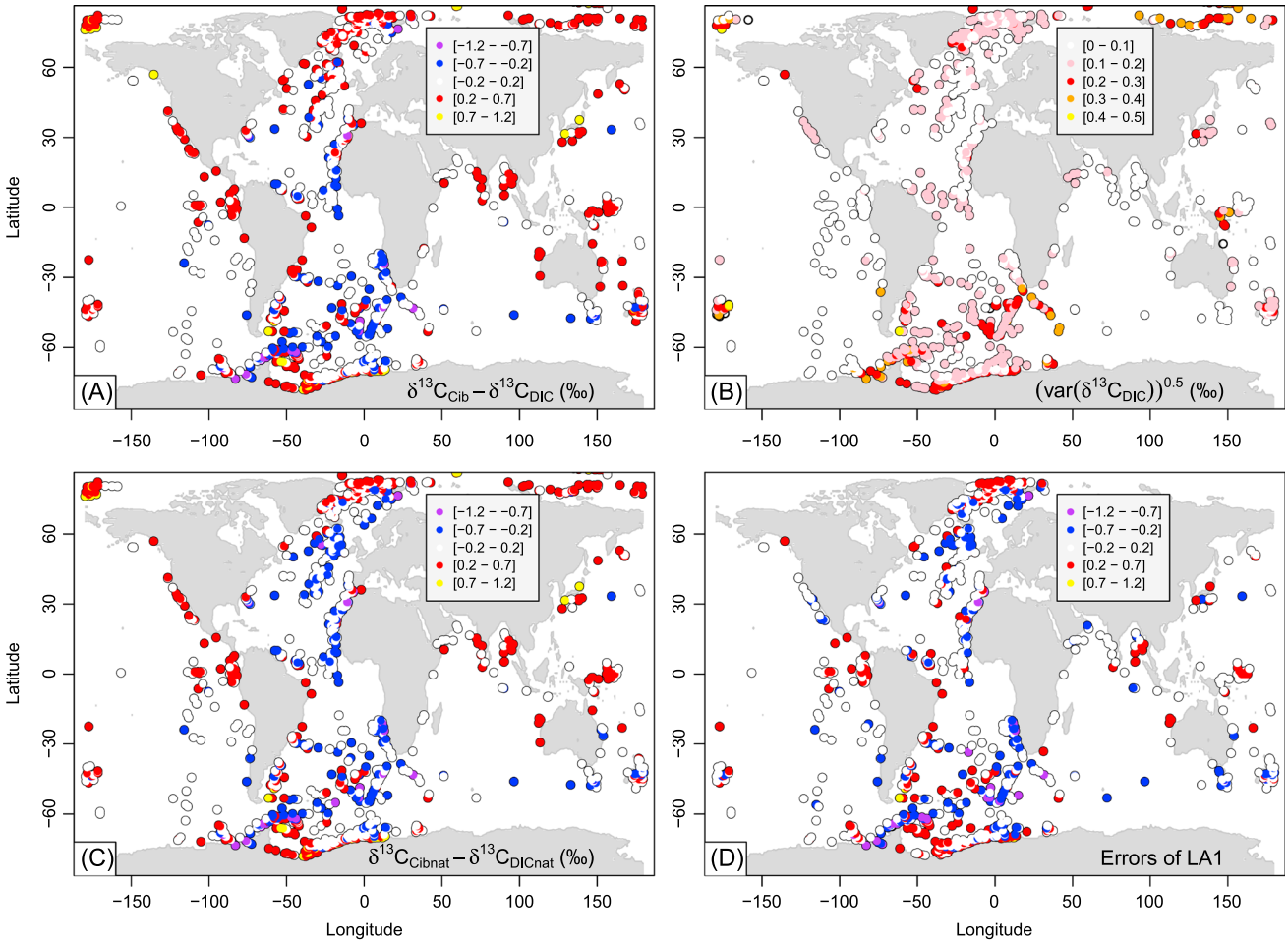

Figure 5. Differences between sediment core top and water column for the (a) raw and (c) anthropogenically corrected data, (b) the standard deviation (square root of the variance) of the water column data mapped onto the locations of the sediment data, and (d) errors of regression LA1 (Table 2). Liberal selection criteria (Δd = 1000 km, $\Delta z = z/5$) were used in all panels.

(Figure 5b). Average standard deviations vary between 0.09 and 0.10‰ for the LH data sets, whereas they are 0.16‰ for M12 and M13. The mean of all data ($\overline{\sigma}_{DICnat} = 0.13$‰) is only one third of $\sigma_{\Delta nat}$, indicating that errors in $\delta^{13}C_{DICnat}$ are a relatively small contribution to Δ_{nat}, although they may affect high latitude data more. Anthropogenic carbon does not affect our estimate of σ_{DICnat} (Figure 4d) because we neglect errors in our estimate of the Suess effect.

The spatial distribution of Δ_{nat} shows mostly positive values in the Arctic, in the Indian and Pacific Oceans, as well as in the Weddell Sea, whereas in the deep Atlantic most values are negative (see also Table S1 and Figure S2 in the SI). In the Atlantic sector of the Southern Ocean negative values coincide with the belt of low $\delta^{13}C_{DIC}$ running east-northeast from Drake Passage (Figures 5c and 6c), consistent with previous observations and perhaps related to the phytodetritus effect [*Mackensen*, 2012; *Mackensen et al.*, 2001, 1993].

3.2. Regression Analyses

In the following we will consider the general, multivariant linear regression model

$$\delta^{13}C_{Cib} = a + b \cdot \delta^{13}C_{DIC} + c \cdot \left[CO_3^{2-}\right] + d \cdot z + \varepsilon, \quad (1)$$

where a is the intercept, b, c, and d are the slopes with respect to $\delta^{13}C_{DIC}$, $[CO_3^{2-}]$ (μM), and depth z (m), and ε is the residual or error. Water depth is included in the regression in order to account for pressure effects. Initially, we had also included temperature on the right-hand side in equation (1), but the results were in

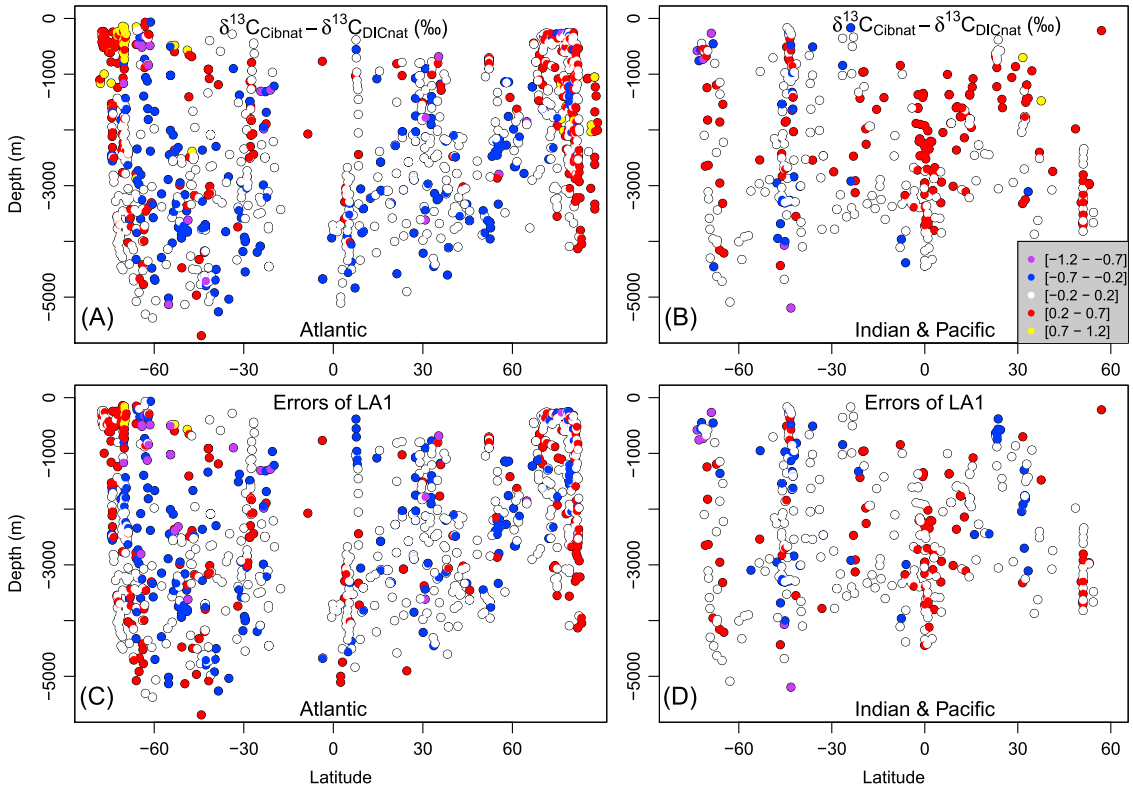

Figure 6. Latitude-depth sections across the (a and c) Atlantic and (b and d) Indian and Pacific of errors using an assumed one-to-one relation (Figures 6a and 6b) and from the multivariant equation (1) with parameters of model LA1 (Table 2 and Figures 6c and 6d).

many cases not statistically significant and resulted in inconsistent signs for the slopes depending on the data sets used (e.g., LH versus All). For these reasons we conclude that we do not find a consistent and statistically significant temperature effect on $\delta^{13}C_{Cib}$ and in the following we do not present results including temperature. Our default case used in most of our regression analyses will set $b = 1$ consistent with theory [*Hesse et al.*, 2014] and because we are unaware of a $\delta^{13}C_{DIC}$-dependent process that would affect fractionation during calcification or vital effects. On the other hand, we are aware and consider $[CO_3^{2-}]$ and pressure (depth)-dependent processes that produce offsets between $\delta^{13}C_{Cib}$ and $\delta^{13}C_{DIC}$ by including coefficients c and d. In order to accommodate situations in which carbonate ion reconstructions are not available we will also consider cases with $b \neq 1$. Since $\sigma_\Delta > \sigma_{DIC}$, it is a reasonable first step to treat $\delta^{13}C_{DIC}$ as the independent, error-free variable. We also assume that the errors associated with $[CO_3^{2-}]$ and z are small and treat them as independent variables.

The resulting statistical parameters including uncertainties are listed in Table 2 for six sets of sensitivity experiments. The six sets differ according to data they include. The first three sets (LA1-LW6) use the liberal selection criterion (L), whereas the remaining three sets (CA1-CW6) use the conservative criterion (C). The first and fourth sets (LA1-LA7 and CA1-CA7) use All data (A), whereas the second and fifth (LL1-LL7 and CL1-CL7) use LH data only (L), and the third and sixth set (LW1, LW5, and LW6 and CW1, CW5, and CW6) use *C. wuellerstorfi* data only (W). Within a given set, up to seven experiments differ only in model assumptions. The first experiment in each set is the default marked in bold in Table 2. It includes carbonate ion and depth in the regression and assumes $b = 1$. Sensitivity experiments 2 and 7 evaluate the effects of not correcting for anthropogenic carbon. Sensitivity experiments 3 and 4 isolate the individual effects of $[CO_3^{2-}]$ and z, respectively, by only including one variable in the regression ($c = 0$ or $d = 0$). Experiment 5 represents the one-to-one relationship ($a = c = d = 0$, $b = 1$). Experiments 6 and 7 allow for $b \neq 1$. Statistical significance for all estimated parameters is evaluated at the 0.01 significance level of the t statistic using the summary(lm) function in *R*.

All default experiments result in significant slopes c for carbonate ion concentrations ranging from -2.2 to -2.9 [10^{-3}‰/(μmol kg^{-1})], with a mean of $-2.6 \pm 0.4 \times 10^{-3}$‰/(μmol kg^{-1}). Experiment 3 in each set, which neglects pressure effects, results in significant and very similar slopes to those of the default experiment

(Figure 8). Slightly shallower slopes with respect to [CO_3^{2-}] result from using All data than using only LH data. The values are of the same order of magnitude but smaller than those measured on planktic foraminifera, which vary between −6 and −14 [10^{-3}‰/(μmol kg^{-1})] for two different species [*Spero et al.*, 1997], but they are larger than theoretical estimates [*Hesse et al.*, 2014], which are around −1 [10^{-3}‰/(μmol kg^{-1})]. To our knowledge, these results provide the first observational, albeit indirect, evidence to suggest that benthic foraminiferal $\delta^{13}C$ is also affected by carbonate ion concentrations.

Consistently negative and significant values are estimated for the slope *d* with respect to depth. For the default experiments using All data (LA1 and CA1) significant values between −0.06 and −0.07‰ km^{-1} are estimated, whereas slopes are smaller if only LH or *C. wuellerstorfi* data are used (−0.03 to −0.05‰ km^{-1}). These numbers are larger than the range of −0.02 to −0.03‰/km suggested by *Hesse et al.* [2014]. Figure 8 suggests that including measurements from shallow depths in the polar data sets (M12 and M13), particularly the M12 data, steepens the slopes. Figure 8 also reveals that the spread of the residuals is larger at shallower depths and decreases with depth, which may reflect increased environmental variability, e.g., of $\delta^{13}C_{DIC}$, in the upper ocean. The larger relative range in the estimated slopes suggests that the pressure effect is more uncertain than the carbonate ion effect. Note that we cannot exclude the possibility that other parameters such as organic matter fluxes may covary with depth and influence the results.

Errors in the default experiments are 0.02 to 0.04‰ smaller than those in experiment 5. This demonstrates that including carbonate ion and pressure effects improves the fit, particularly for LH and *C. wuellerstorfi* data for which the relative error reduction is larger (12–17%) than for All data (6–10%). This conclusion is also supported by additional tests (not shown) in which experiment 5 was repeated for each set but allowing for an intercept in the regression ($a \neq 0$), the results of which were very similar. Examining experiments 3 and 4 reveals that including carbonate ion has larger effects than depth on reducing the residual errors for LH data, whereas for All data the effects of including depth are similar to those for [CO_3^{2-}].

Allowing for $b \neq 1$ in experiment 6 results in estimated values for *b* between 0.74 and 0.89. Not including carbonate ion in these models causes the slope *b* to be lower than one because carbonate ion and $\delta^{13}C_{DIC}$ distributions in the ocean are highly correlated (e.g., compare Figure 2b with Figure 3d) due to the remineralization of organic matter. Linear regressions of $[CO_3^{2-}] = A + B \cdot \delta^{13}C_{DIC}$ using our data over all depths yield correlation coefficients between 0.64 and 0.80 and values for $B = \Delta[CO_3^{2-}]/\Delta\delta^{13}C_{DIC}$ of 56 and 68 (μmol kg^{-1})/‰ for All and LH, respectively, somewhat larger than what *Yu et al.* [2008] report for deep waters (43 (μmol kg^{-1})/‰). Using these numbers to replace [CO_3^{2-}] in equation (1) and our range for *c* of −2.2 to −2.9 [10^{-3}‰/(μmol kg^{-1})] as estimated from the default models yields a decrease of *b* by $\Delta b = B \cdot c$ from −0.12 to −0.19‰, which explains most, if not all, of the deviations of *b* from unity. Additional sensitivity experiments (not shown) confirm interactions between *b* and *c*. E.g., assuming a fixed $c = -0.01$‰/(μmol kg^{-1}) as measured in planktic foraminifera [*Spero et al.*, 1997] in a repeat of experiment LL7 results in $b = 1.4$ and slightly increases the residuals to 0.28‰. Assuming $c = -0.01$‰/(μmol kg^{-1}) and $b = 1$ in a repeat of experiment LL1 increases the residuals substantially to 0.34‰. These results also suggest that the carbonate ion effect among *Cibicides* growing in their natural habitat is smaller ($c > -0.003$‰/(μmol kg^{-1})) than that found by *Spero et al.* [1997] in laboratory cultures of planktic foraminifera.

Anthropogenic effects considerably affect the estimated parameters. Comparing experiment 2 with the default experiments indicates that if anthropogenic effects are not removed, the slopes of the carbonate ion effect are underestimated (too shallow), whereas the slopes for depth are overestimated (too steep). Comparison of experiments 6 and 7 demonstrates that not accounting for the Suess effect leads to lower correlation coefficients, can increase residuals, and overestimates slopes *b* for $\delta^{13}C_{DIC}$ because $\delta^{13}C_{DIC}$ values in the high range (North Atlantic) are decreased (pulled toward the left in Figure 7).

Estimated regression parameters are very similar regardless of whether the liberal or conservative selection criterion is used, and in many cases they are indistinguishable. The correlation coefficients are slightly larger for the conservative criterion, and the slopes for carbonate ion are slightly steeper. These similarities suggest that the results are robust with respect to the selection criterion.

Differences between All and LH or *C. wuellerstorfi* only data are more substantial. For experiments 6 and 7 using only LH or *C. wuellerstorfi* data leads to shallower slopes *b* compared with All. This is due to the removal of the Arctic measurements, which plot systematically higher than the LH data in Figure 7 (bright green dots). This is consistent with the finding by *Mackensen* [2013] that the Arctic foraminiferal data are about 0.2‰ higher than

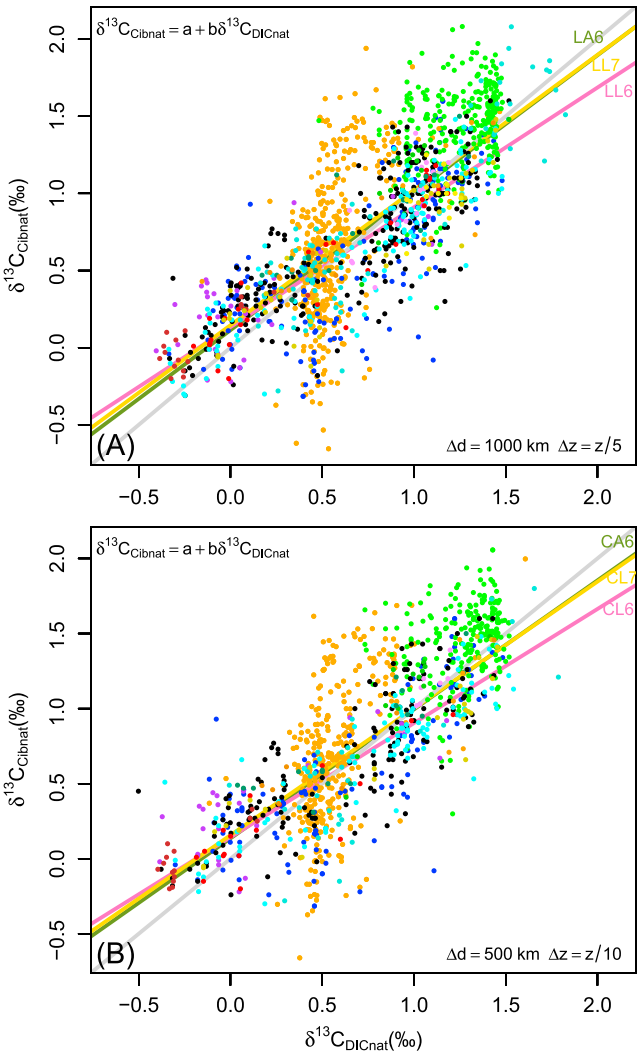

Figure 7. Water column versus sediment $\delta^{13}C$ data using (a) liberal (Δd = 1000 km; $\Delta z = z/5$) and (b) conservative (Δd = 500 km; $\Delta z = z/10$) spatial matching criteria. Different data sets are indicated by dots using the same color scheme as in Figure 1. The one-to-one line is shown in grey. Olive green lines indicate results of linear regressions using All data (LA6 and CA6), whereas hot pink and gold lines indicate results using only Late Holocene data (LL6 and CL6). Golden lines apply no correction for the Suess effect (LL7 and CL7), which leads to steeper slopes compared to corrected data (LL6, CL6, hot pink). Regression parameters are listed in Table 2.

$\delta^{13}C_{DIC}$. Note that this bias in the one-to-one relation is strongly reduced in the multi-variate regressions (e.g., LA1 versus LA5 in Table 3) suggesting that carbonate ion and/or depth effects are responsible for creating it.

More generally, the LH and *C. wuellerstorfi* data show consistently smaller residuals (σ = 0.21 to 0.25‰) than All data (σ = 0.29‰). As shown in Figure 9 and Table 3, this is mainly due to the inclusion of the M12 Antarctic data, which have errors (0.35–0.42‰) that are consistently larger than those of the other data sets, which are typically between 0.2 and 0.3‰. The contemporary Arctic *Cibicides* data (M13) have residuals more consistent with the LH data than with M12. This does not support the idea that the larger spread in the M12 data is due to the smaller number of individual shells measured compared with the LH data. Negative deviations in the Southern Ocean could be explained by the phytodetritus effect [*Mackensen*, 2012; *Mackensen et al.*, 2001, 1993] or occasional infaunal habitat of some species such as *C. kullenbergi* [*Gottschalk et al.*, 2016], which are included in M12. However, the question arises what causes the positive deviations there. Figures 8 and S2 indicate that positive deviations in M12 are mainly from shallow depths, which may be dispropotionally influenced by temporal variability. Thus, the relatively large amount of data from shallow depths could contribute to the larger errors for M12. Our approach of assessing $\delta^{13}C_{DIC}$ at the sites of the sediment data does not account for temporal (e.g., seasonal) or small-scale spatial heterogeneities that may impact benthic $\delta^{13}C_{DIC}$ particularly in the South Atlantic [*Mackensen*, 2012; *Mackensen and Bickert*, 1999]. Errors for C10 (0.32–0.34‰) are larger than those of the other LH data sets, perhaps due to the less well-constrained ages of those samples.

Including carbonate ion and depth in the regression reduces the residuals for most data subsets (Table 3 and Figure 9) and in most regions (see SI Table S1 and Figure S2). The improvement is largest for the tropical and extratropical North Pacific, the Indian, the Arctic, and the Antarctic for which positive biases are strongly reduced, and for the North Atlantic, where negative biases are reduced. The one-to-one relationship provides a marginally better fit in the South Pacific and the tropical West Atlantic. The southeast Pacific, South Atlantic, and Antarctic are the regions with the largest errors for model LA1 (Table S1). Not many data are available from the southeast Pacific, hampering the assessment there.

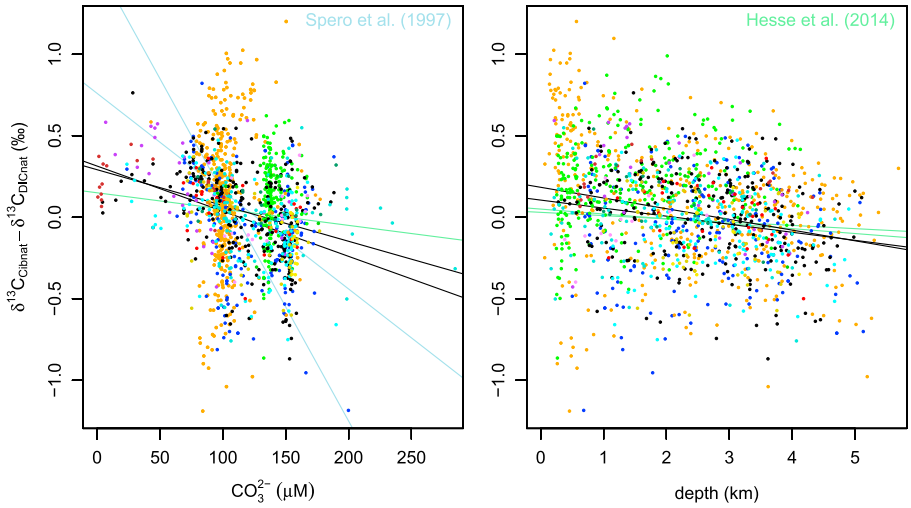

Figure 8. Foraminifera − water column $\delta^{13}C$ difference versus water column (left) [CO_3^{2-}] and (right) depth. Color symbols as in Figure 1. Black lines, which are the slopes from our regression analyses LA3, LA4, LL3, and LL4, are compared to results from *Spero et al.* [1997] (light blue) and *Hesse et al.* [2014] (light green).

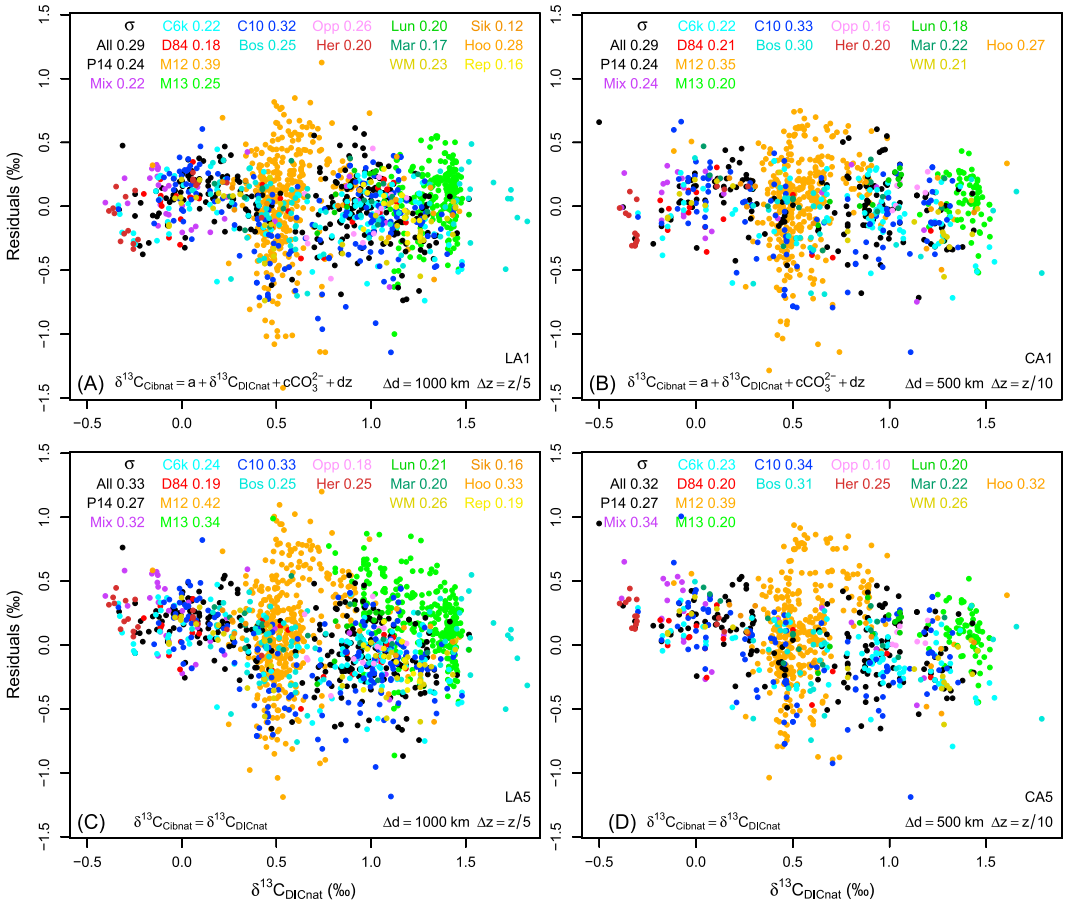

Figure 9. Fitted values ($\delta^{13}C_{Cibnat}$) versus residuals for different linear regression models (indicated at the bottom left) and different spatial selection criteria (indicated in the bottom right corner. Color scheme as in Figure 1. Numbers in the upper parts of each panel indicate the standard deviations of all data (All) and the individual data sets (see Table 1 for abbreviations).

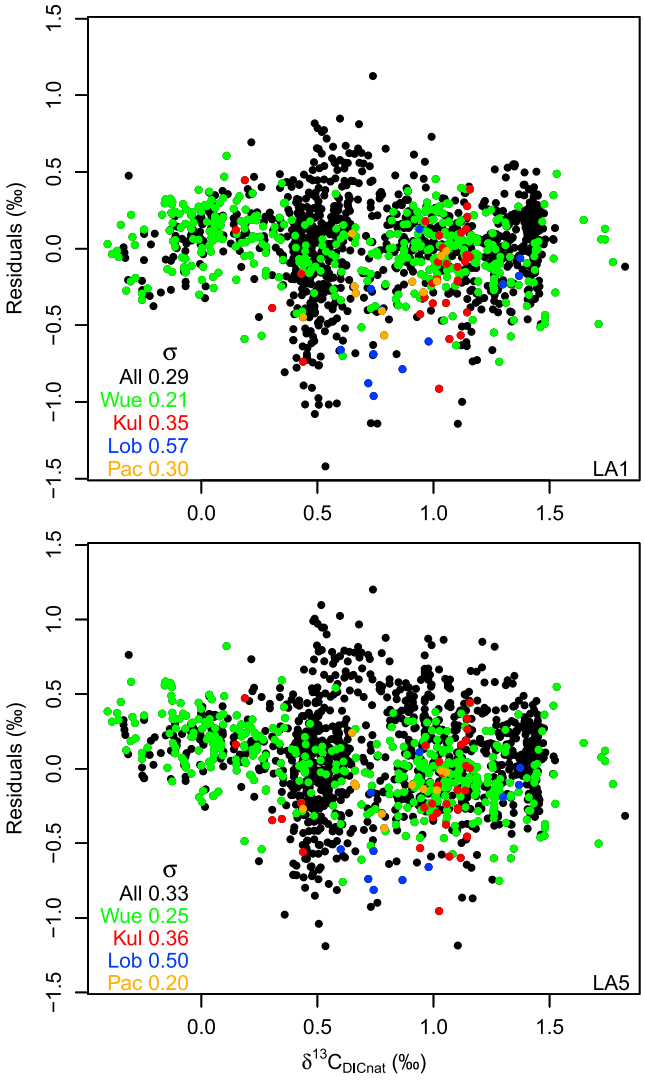

Figure 10. As Figure 9 but for different species: *Cibicides wuellerstorfi* (Wue, green), *Cibicides kullenbergi* (Kul, red), *Cibicides lobatulus* (Lob, blue), and *Cibicides pachyderma* (Pac, orange).

The South Atlantic shows interesting zonal differences. Errors are larger in the southeast Atlantic where foraminifera-based estimates suffer from a substantial negative bias of −0.18‰, whereas in the southwest Atlantic their bias is smaller and positive (+0.07‰). Note that these biases exacerbate the zonal difference from less than 0.2‰ in the water column to more than 0.4‰ in the forminifera-based estimates.

Using the more conservative spatial matching criteria reduces the residuals in some cases (M13 and Opp), which indicates that errors in $\delta^{13}C_{DIC}$ do affect the results, but the overall effect appears to be relatively small.

Using only data from *C. wuellerstorfi* (models LW and CW in Table 2 and Wue in Table 3) results in similar estimated parameters and errors than LH, which is not surprising given that most LH data are presumably *C. wuellerstorfi*. However, *C. kullenbergi*, *C. lobatulus*, and *C. pachyderma* result in mostly larger errors and biases (Table 3 and Figure 10). This is particularly true for *C. lobatulus*, which suffers from a large negative bias, consistent with earlier findings [*Mackensen and Licari*, 2004; *Murray*, 2006]. However, note that our comparison may be compromised by the small amout of data for species other than *C. wuellerstorfi*.

4. Discussion

Having established that both carbonate ion and pressure effects impact benthic carbon isotopes and that considering these effects improves the fit and reduces errors and regional biases, we recommend equation (1) with parameters as in LA1 or some of the other default models to estimate $\delta^{13}C_{DIC}$ from $\delta^{13}C_{Cib}$ if $[CO_3^{2-}]$ has also been reconstructed (water depth is usually known). Recently developed methods to reconstruct $[CO_3^{2-}]$ concentrations such as those based on B/Ca ratios [*Yu and Elderfield*, 2007] may be useful. If $[CO_3^{2-}]$ reconstructions are not available, we suggest using LA6, LL6, LW6, CA6, CL6, or CW6, which would consider at least the modern observed correlation between $[CO_3^{2-}]$ and $\delta^{13}C_{DIC}$. In model studies simulated $\delta^{13}C_{DIC}$, $[CO_3^{2-}]$ concentrations and depth can be used to estimate $\delta^{13}C_{Cib}$, which can then be compared to observations.

Implications of pH and temperature effects on glacial-interglacial $\delta^{13}C_{DIC}$ reconstructions have been discussed previously in *Hesse et al.* [2014] who found a strong temperature effect that suggests that 0.11‰ of the observed total whole ocean ~0.35‰ $\delta^{13}C_{Cib}$ drop from the interglacial to the glacial ocean could be

explained by a cooling of bottom waters by 2.5°C. Our analysis did not result in a consistent significant temperature effect, thus questioning their conclusion.

Our results have implications for glacial-interglacial $\delta^{13}C$ reconstructions. Carbonate ion concentrations were similar in the Pacific and Indian oceans but about 20 μmol kg^{-1} lower in the deep Atlantic and 20 to 30 μmol kg^{-1} higher in the upper Atlantic during the LGM compared to the preindustrial ocean [*Allen et al.*, 2015; *Gottschalk et al.*, 2015; *Yu et al.*, 2008, 2013, 2014]. Using equation (1) with $c = -2.6 \times 10^{-3}$‰/(μmol kg^{-1}), this would produce a 0.05‰ reduction in $\delta^{13}C_{DIC}$ in the deep Atlantic and an increase of 0.05–0.08‰ in the upper Atlantic, thereby slightly enhancing the observed interglacial-to-glacial increase in the vertical gradient of ~1.0‰ in $\delta^{13}C_{Cib}$ [*Yu et al.*, 2008, Figure 4].

Our finding that biases in the South Atlantic exacerbate the zonal gradient in $\delta^{13}C_{DIC}$ there may also explain the large zonal gradients found in glacial reconstructions there [*Hodell et al.*, 2003; *Hoffman and Lund*, 2012; *Waelbroeck et al.*, 2011] and questions their reliability, particularly those from the southeast Atlantic where $\delta^{13}C_{Cib}$ exhibits large negative biases compared with $\delta^{13}C_{DIC}$ regardless of whether carbonate ion and pressure effects are considered or not (Table S1). The ultimate reasons for these biases as well as the large errors in the Antarctic remain open questions.

Remaining errors may be influenced by accumulation rates. In low accumulation rate cores, bioturbation may cause contamination of surface sediments with older glacial or deglacial material. Currently, accumulation rate information is not available in our data set, but it would be desirable to include it in the future in order to evaluate this issue. Future updates of the database with more consistent species, core top dating, and coring equipment information and analyzing if and how residuals are affected will be another useful effort.

5. Summary and Conclusions

Our synthesis of late Holocene core top $\delta^{13}C_{Cib}$ data includes more than an order of magnitude more measurements than that used in the previous global calibration of D84. This, together with the vastly enhanced database of water column $\delta^{13}C_{DIC}$ measurements, has prompted a new global calibration of $\delta^{13}C_{Cib}$. The results confirm the strong correlation between $\delta^{13}C_{Cib}$ and $\delta^{13}C_{DIC}$ found by D84. However, we show that results of regression analyses are impacted by the invasion of ^{13}C-depleted, anthropogenic carbon and indicate statistically significant secondary effects from carbonate ion and pressure. Including these secondary effects improves the estimation of $\delta^{13}C_{DIC}$ by reducing systematic regional biases, errors and by increasing correlation. We therefore recommend using equation (1) with parameters LA1 (Table 2) rather than a simple one-to-one relationship between $\delta^{13}C_{DIC} \approx \delta^{13}C_{Cib}$. The regression coefficients with respect to carbonate ion and pressure are qualitatively consistent with previous theoretical [*Hesse et al.*, 2014] and experimental [*Spero et al.*, 1997] studies, but quantitatively, the carbonate ion effects are smaller than those of *Spero et al.* [1997] and larger than those of *Hesse et al.* [2014], respectively. Hence, these secondary effects are relatively small and would in practical applications modify reconstructed $\delta^{13}C_{DIC}$ changes by typically less than about 15% compared to the often used one-to-one relationship. For most individual downcore records, *z* is practically invariant and carbonate ion varies relatively little, so that they will have limited impact on reconstructions of temporal variability. Thus, most conclusions of previous studies assuming a one-to-one relationship remain likely robust.

We find errors are typically 0.2–0.3‰, although they are larger in the southeast Atlantic and Antarctic (~0.4‰) and larger in the upper ocean than at depths. We find lower errors for *C. wuellerstorfi* and higher errors and negative biases for *C. lobatulus* compared with *C. kullenbergi* and *C. pachyderma*, consistent with *Mackensen and Licari* [2004] and *Murray* [2006] who also indicate lower $\delta^{13}C$ values for *C. lobatulus*. These errors are larger than the 0.15‰ reported by D84. Future efforts could be directed toward understanding the sources for the remaining errors, such as a more comprehensive analysis of species offsets, information on size and number of shells measured, coring equipment used, sediment type and accumulation rates, age constraints, and temporal variability of $\delta^{13}C_{DIC}$ and $\delta^{13}C_{Cib}$, so as to be able to improve the use of $\delta^{13}C$ as a paleoceanographic proxy. This will require updating and extending the database to include relevant but currently missing information.

Acknowledgments
We thank Matthew P. Humphreys for noting a duplicate cruise in the S13 data set, which we subsequently removed. OC3 is supported by PAGES, a core project of Future Earth. PAGES is supported by the U.S. and Swiss National Science Foundations. Support for this project was also provided by the U.S. National Science Foundation (award 1634719 to A.S. and A.C.M., awards 0926735 and 1125181 to L.E.L. and C.D.P., and award OCE-1003500 to D.C.L.), the Swiss National Science Foundation (awards PP00P2_144811 and 200021_163003 to S.L.J.), the Canadian Institute for Advanced Research (CIFAR), the Canadian Foundation for Innovation (CFI), and the Natural Sciences and Engineering Research Council (NSERC). Authors of newly presented data in this paper express their gratitude to the various ship expedition parties and chief scientists for making material available (SO228, SO245, MSM48, and M124). Data used are listed in the references, tables, and supplements and available at NOAA's Paleoclimate repository at https://www.ncdc.noaa.gov/paleo-search/study/21750 (water column data) and https://www.ncdc.noaa.gov/paleo-search/study/22110 (sediment core top data).

References

Allen, K. A., E. L. Sikes, B. Honisch, A. C. Elmore, T. P. Guilderson, Y. Rosenthal, and R. F. Anderson (2015), Southwest Pacific deep water carbonate chemistry linked to high southern latitude climate and atmospheric CO_2 during the Last Glacial Termination, *Quat. Sci. Rev.*, *122*, 180–191.

Belanger, P. E., W. B. Curry, and R. K. Matthews (1981), Core-top evaluation of benthic foraminiferal isotopic-ratios for paleo-oceanographic interpretations, *Palaeogeogr. Palaeoclimatol. Palaeoecol.*, *33*, 205–220.

Bernhard, J. M., D. R. Ostermann, D. S. Williams, and J. K. Blanks (2006), Comparison of two methods to identify live benthic foraminifera: A test between Rose Bengal and CellTracker Green with implications for stable isotope paleoreconstructions, *Paleoceanography*, *21*, PA4210, doi:10.1029/2006PA001290.

Böhm, F., A. Haase-Schramm, A. Eisenhauer, W. C. Dullo, M. M. Joachimski, H. Lehnert, and J. Reitner (2002), Evidence for preindustrial variations in the marine surface water carbonate system from coralline sponges, *Geochem. Geophys. Geosyst.*, *3*(3), doi:10.1029/2001GC000264.

Broecker, W. S. (1982), Glacial to interglacial changes in ocean chemistry, *Prog. Oceanogr.*, *11*, 151–197.

Charles, C. D., and R. G. Fairbanks (1990), Glacial to interglacial changes in the isotopic gradients of Southern Ocean surface water, in *Geological History of the Polar Oceans: Arctic Versus Antarctic*, edited by U. Bleil and J. Thiede, pp. 519–538, Springer, Netherlands.

Corliss, B. H. (1985), Microhabitats of benthic foraminifera within deep-sea sediments, *Nature*, *314*, 435–438.

Cortese, G., and J. Prebble (2015), A radiolarian-based modern analogue dataset for palaeoenvironmental reconstructions in the southwest Pacific, *Mar. Micropaleontol.*, *118*, 34–49.

Curry, W. B., and D. W. Oppo (2005), Glacial water mass geometry and the distribution of delta C-13 of Sigma CO_2 in the western Atlantic Ocean, *Paleoceanography*, *20*, PA1017, doi:10.1029/2004PA001021.

Duplessy, J. C., N. J. Shackleton, R. K. Matthews, W. Prell, W. F. Ruddiman, M. Caralp, and C. H. Hendy (1984), C-13 record of benthic foraminifera in the last interglacial ocean—Implications for the carbon-cycle and the global deep-water circulation, *Quat. Res.*, *21*, 225–243.

Duplessy, J. C., N. J. Shackleton, R. G. Fairbanks, L. Labeyrie, D. Oppo, and N. Kallel (1988), Deepwater source variations during the last climatic cycle and their impact on the global deepwater circulation, *Paleoceanography*, *3*, 343–360.

Fontanier, C., A. Mackensen, F. J. Jorissen, P. Anschutz, L. Licari, and C. Griveaud (2006), Stable oxygen and carbon isotopes of live benthic foraminifera from the Bay of Biscay: Microhabitat impact and seasonal variability, *Mar. Micropaleontol.*, *58*, 159–183.

Gebbie, G. (2014), How much did glacial North Atlantic water shoal?, *Paleoceanography*, *29*, 190–209, doi:10.1002/2013PA002557.

Gottschalk, J., L. C. Skinner, S. Misra, C. Waelbroeck, L. Menviel, and A. Timmermann (2015), Abrupt changes in the southern extent of North Atlantic Deep Water during Dansgaard-Oeschger events, *Nat. Geosci.*, *8*, 950–U986.

Gottschalk, J., N. Vázquez Riveiros, C. Waelbroeck, L. C. Skinner, E. Michel, J. C. Duplessy, D. A. Hodell, and A. Mackensen (2016), Carbon isotope offsets between benthic foraminifer species of the genus Cibicides (Cibicidoides) in the glacial sub-Antarctic Atlantic, *Paleoceanography*, *31*, 1583–1602, doi:10.1002/2016PA003029.

Gruber, N., C. D. Keeling, R. B. Bacastow, P. R. Guenther, T. J. Lueker, M. Wahlen, H. A. J. Meijer, W. G. Mook, and T. F. Stocker (1999), Spatiotemporal patterns of carbon-13 in the global surface oceans and the oceanic Suess effect, *Global Biogeochem. Cycles*, *13*, 307–335.

Herguera, J. C., T. Herbert, M. Kashgarian, and C. Charles (2010), Intermediate and deep water mass distribution in the Pacific during the Last Glacial Maximum inferred from oxygen and carbon stable isotopes, *Quat. Sci. Rev.*, *29*, 1228–1245.

Hesse, T., D. Wolf-Gladrow, G. Lohmann, J. Bijma, A. Mackensen, and R. E. Zeebe (2014), Modelling delta C-13 in benthic foraminifera: Insights from model sensitivity experiments, *Mar. Micropaleontol.*, *112*, 50–61.

Hodell, D. A., C. D. Charles, and F. J. Sierro (2001), Late Pleistocene evolution of the ocean's carbonate system, *Earth Planet. Sci. Lett.*, *192*, 109–124.

Hodell, D. A., K. A. Venz, C. D. Charles, and U. S. Ninnemann (2003), Pleistocene vertical carbon isotope and carbonate gradients in the South Atlantic sector of the Southern Ocean, *Geochem. Geophys. Geosyst.*, *4*(1), 1004, *doi:*10.1029/2002GC000367.

Hoffman, J. L., and D. C. Lund (2012), Refining the stable isotope budget for Antarctic Bottom Water: New foraminiferal data from the abyssal Southwest Atlantic, *Paleoceanography*, *27*, PA1213, doi:10.1029/2011PA002216.

Hoogakker, B. A. A., M. R. Chapman, I. N. McCave, C. Hillaire-Marcel, C. R. W. Ellison, I. R. Hall, and R. J. Telford (2011), Dynamics of North Atlantic deep water masses during the holocene, *Paleoceanography*, *26*, PA4214, doi:10.1029/2011PA002155.

Ishimura, T., U. Tsunogai, S. Hasegawa, S. Hasegawa, T. Oi, H. Kitazato, H. Suga, and T. Toyofuku (2012), Variation in stable carbon and oxygen isotopes of individual benthic foraminifera: Tracers for quantifying the magnitude of isotopic disequilibrium, *Biogeosciences*, *9*, 4353–4367.

Jorissen, F. J., H. C. de Stigter, and J. G. V. Widmark (1995), A conceptual model explaining benthic foraminiferal microhabitats, *Mar. Micropaleontol.*, *26*, 3–15.

Keeling, C. D. (1979), The Suess effect: ^{13}Carbon-^{14}Carbon interrelations, *Environ. Int.*, *2*, 229–300.

Key, R. M., A. Kozyr, C. L. Sabine, K. Lee, R. Wanninkhof, J. L. Bullister, R. A. Feely, F. J. Millero, C. Mordy, and T.-H. Peng (2004), A global ocean carbon climatology: Results from global data analysis project (GLODAP), *Global Biogeochem. Cycles*, *18*, GB4031, doi:10.1029/2004GB002247.

Khatiwala, S., F. Primeau, and T. Hall (2009), Reconstruction of the history of anthropogenic CO_2 concentrations in the ocean, *Nature*, *462*, 346–U110.

Kroopnick, P. M. (1985), The distribution of C-13 of Sigma-CO_2 in the World oceans, *Deep Sea Res., Part A*, *32*, 57–84.

Locarnini, R. A., A. V. Mishonov, J. I. Antonov, T. P. Boyer, and H. E. Garcia (2006), *World Ocean Atlas 2005, Volume 1: Temperature*, *NOAA Atlas NESDIS 61*, edited by S. Levitus, pp. 1–182, U.S. Gov. Print. Off., Washington, D. C.

Lund, D. C., A. C. Tessin, J. L. Hoffman, and A. Schmittner (2015), Southwest Atlantic watermass evolution during the last deglaciation, *Paleoceanography*, *30*, 477–494, doi:10.1002/2014PA002657.

Lutze, G. F., and H. Thiel (1989), Epibenthic foraminifera from elevated microhabitats; Cibicidoides wuellerstorfi and *Planulina ariminensis*, *J. Foramin. Res.*, *19*, 153.

Lynch-Stieglitz, J., M. W. Schmidt, L. Gene Henry, W. B. Curry, L. C. Skinner, S. Mulitza, R. Zhang, and P. Chang (2014), Muted change in Atlantic overturning circulation over some glacial-aged Heinrich events, *Nat. Geosci.*, *7*, 144–150.

Mackensen, A. (2012), Strong thermodynamic imprint on recent bottom-water and epibenthic delta C-13 in the Weddell Sea revealed: Implications for glacial Southern Ocean ventilation, *Earth Planet. Sci. Lett.*, *317*, 20–26.

Mackensen, A. (2013), High epibenthic foraminiferal delta C-13 in the recent deep Arctic Ocean: Implications for ventilation and brine release during stadials, *Paleoceanography*, *28*, 574–584, doi:10.1002/palo.20058.

Mackensen, A., and T. Bickert (1999), Stable carbon isotopes in benthic foraminifera: Proxies for deep and bottom water circulation and new production, in *Use of Proxies in Paleoceanography: Examples From the South Atlantic*, edited by G. Fischer and G. Wefer, pp. 229–254, Springer, Berlin, Heidelberg.

Mackensen, A., and L. Licari (2004), Carbon isotopes of live benthic foraminifera from the South Atlantic: Sensitivity to bottom water carbonate saturation state and organic matter rain rates, in *The South Atlantic in the Late Quaternary*, edited by G. Wefer, S. Mulitza, and V. Ratmeyer, pp. 623–644, Springer, Berlin, Heidelberg.

Mackensen, A., H. W. Hubberten, T. Bickert, G. Fischer, and D. K. Fuetterer (1993), The δ13C in benthic foraminiferal tests of Fontbotia wuellerstorfi (Schwager) relative to the δ13C of dissolved inorganic carbon in Southern Ocean Deep Water: Implications for glacial ocean circulation models, *Paleoceanography*, *8*, 587–610.
Mackensen, A., M. Rudolph, and G. Kuhn (2001), Late Pleistocene deep-water circulation in the subantarctic eastern Atlantic, *Global Planet. Change*, *30*, 197–229.
Marchal, O., and W. B. Curry (2008), On the abyssal circulation in the glacial Atlantic, *J. Phys. Oceanogr.*, *38*, 2014–2037.
Martínez-Méndez, G., D. Hebbeln, M. Mohtadi, F. Lamy, R. D. Pol-Holz, D. Reyes-Macaya, and T. Freudenthal (2013), Changes in the advection of Antarctic Intermediate Water to the northern Chilean coast during the last 970 kyr, *Paleoceanography*, *28*, 607–618, doi:10.1002/palo.20047.
McCorkle, D. C., S. R. Emerson, and P. D. Quay (1985), Stable carbon isotopes in marine porewaters, *Earth Planet. Sci. Lett.*, *74*, 13–26.
McCorkle, D. C., L. D. Keigwin, B. H. Corliss, and S. R. Emerson (1990), The influence of microhabitats on the carbon isotopic composition of deep-sea benthic foraminifera, *Paleoceanography*, *5*, 161–185.
Murray, J. W. (2006), *Ecology and Applications of Benthic Foraminifera*, pp. 1–426, Cambridge Univ. Press, Cambridge, U. K.
Olsen, A., and U. Ninnemann (2010), Large delta C-13 gradients in the preindustrial North Atlantic revealed, *Science*, *330*, 658–659.
Peterson, C. D., L. E. Lisiecki, and J. V. Stern (2014), Deglacial whole-ocean delta C-13 change estimated from 480 benthic foraminiferal records, *Paleoceanography*, *29*, 549–563, doi:10.1002/2013PA002552.
Prebble, J. G., E. M. Crouch, L. Carter, G. Cortese, H. Bostock, and H. Neil (2013), An expanded modern dinoflagellate cyst dataset for the Southwest Pacific and Southern Hemisphere with environmental associations, *Mar. Micropaleontol.*, *101*, 33–48.
Quay, P., and J. Wu (2015), Impact of end-member mixing on depth distributions of $\delta^{13}C$, cadmium and nutrients in the N. Atlantic Ocean, *Deep Sea Res., Part II*, *116*, 107–116.
Rathburn, A. E., B. H. Corliss, K. D. Tappa, and K. C. Lohmann (1996), Comparisons of the ecology and stable isotopic compositions of living (stained) benthic foraminifera from the Sulu and South China Seas, *Deep Sea Res., Part I*, *43*, 1617–1646.
Schmiedl, G., M. Pfeilsticker, C. Hemleben, and A. Mackensen (2004), Environmental and biological effects on the stable isotope composition of recent deep-sea benthic foraminifera from the western Mediterranean Sea, *Mar. Micropaleontol.*, *51*, 129–152.
Schmittner, A., N. Gruber, A. C. Mix, R. M. Key, A. Tagliabue, and T. K. Westberry (2013), Biology and air-sea gas exchange controls on the distribution of carbon isotope ratios ($\delta^{13}C$) in the ocean, *Biogeosciences*, *10*, 5793–5816.
Schweizer, M., J. Pawlowski, T. Kouwenhoven, and B. van der Zwaan (2009), Molecular phylogeny of common cibicidids and related rotaliida (foraminifera) based on small subunit rDNA sequences, *J. Foraminifer. Res.*, *39*, 300.
Shackleton, N. J. (1977), Carbon-13 in Uvigerina: Tropical rainforest history and the Equatorial Pacific carbonate dissolution cycles, in *The Fate of Fossil Fuel CO2 in the Oceans*, edited by N. R. Andersen, and A. Malahoff, pp. 401–427, Plenum, New York.
Spero, H. J., J. Bijma, D. W. Lea, and B. E. Bemis (1997), Effect of seawater carbonate concentration on foraminiferal carbon and oxygen isotopes, *Nature*, *390*, 497–500.
Suess, H. E. (1955), Radiocarbon concentration in modern wood, *Science*, *122*, 415.
Tachikawa, K., and H. Elderfield (2002), Microhabitat effects on Cd/Ca and delta C-13 of benthic foraminifera, *Earth Planet. Sci. Lett.*, *202*, 607–624.
Waelbroeck, C., C. Skinner, L. Labeyrie, J.-C. Duplessy, E. Michel, N. Vazquez Riveiros, J.-M. Gherardi, and F. Dewilde (2011), The timing of deglacial circulation changes in the Atlantic, *Paleoceanography*, *26*, PA3213, doi:10.1029/2010PA002007.
Weinelt, M., et al. (2001), Paleoceanographic proxies in the northern North Atlantic, in *The Northern North Atlantic: A Changing Environment*, edited by P. Schäfer et al., pp. 319–352, Springer, Berlin, Heidelberg.
Wollenburg, J. E., M. Raitzsch, and R. Tiedemann (2015), Novel high-pressure culture experiments on deep-sea benthic foraminifera—Evidence for methane seepage-related $\delta^{13}C$ of *Cibicides wuellerstorfi*, *Mar. Micropaleontol.*, *117*, 47–64.
Yu, J. M., and H. Elderfield (2007), Benthic foraminiferal B/Ca ratios reflect deep water carbonate saturation state, *Earth Planet. Sci. Lett.*, *258*, 73–86.
Yu, J. M., H. Elderfield, and A. M. Piotrowski (2008), Seawater carbonate ion-delta C-13 systematics and application to glacial-interglacial North Atlantic ocean circulation, *Earth Planet. Sci. Lett.*, *271*, 209–220.
Yu, J. M., R. F. Anderson, Z. D. Jin, J. W. B. Rae, B. N. Opdyke, and S. M. Eggins (2013), Responses of the deep ocean carbonate system to carbon reorganization during the Last Glacial–interglacial cycle, *Quat. Sci. Rev.*, *76*, 39–52.
Yu, J. M., R. F. Anderson, Z. D. Jin, L. Menviel, F. Zhang, F. J. Ryerson, and E. J. Rohling (2014), Deep South Atlantic carbonate chemistry and increased interocean deep water exchange during last deglaciation, *Quat. Sci. Rev.*, *90*, 80–89.
Zahn, R., K. Winn, and M. Sarnthein (1986), Benthic foraminiferal $\delta^{13}C$ and accumulation rates of organic carbon: *Uvigerina peregrina* Group and Cibicidoides Wuellerstorfi, *Paleoceanography*, *1*, 27–42.
Zahn, R., M. Sarnthein, and H. Erlenkeuser (1987), Benthic isotope evidence for changes of the Mediterranean outflow during the Late Quaternary, *Paleoceanography*, *2*(6), 543–559, doi:10.1029/PA002i006p00543.
Zeebe, R. E., and D. A. Wolf-Gladrow (2001), *CO_2 in Seawater: Equilibrium, Kinetics, Isotopes*, vol. 65, pp. 1–360, Elsevier, Amsterdam.

Erratum

In the originally published version of this manuscript, line 9 of the abstract contained an error. The number 10^{-3} should be replaced by 10^{-5}. Additionally, links provided in the acknowledgment section are inoperable.

The following should be used:

https://www.ncdc.noaa.gov/paleo-search/study/22110
https://www.ncdc.noaa.gov/paleo-search/study/21750

These errors have since been corrected, and this version may be considered the authoritative version of record.